

See discussions, stats, and author profiles for this publication at: <https://www.researchgate.net/publication/271383683>

Behavior of Tin-Based “Super-POSS” Incorporated in Different Bonding Situations in Hybrid Epoxy Resins

ARTICLE in MACROMOLECULES · JULY 2014

Impact Factor: 5.8 · DOI: 10.1021/ma500507j

CITATIONS

2

READS

26

7 AUTHORS, INCLUDING:



François Ribot

Pierre and Marie Curie University - Paris 6

108 PUBLICATIONS 3,826 CITATIONS

[SEE PROFILE](#)



Miroslava Trchová

Academy of Sciences of the Czech Republic

174 PUBLICATIONS 5,769 CITATIONS

[SEE PROFILE](#)



Milos Steinhart

Academy of Sciences of the Czech Republic

59 PUBLICATIONS 604 CITATIONS

[SEE PROFILE](#)



Ewa Pavlova

Academy of Sciences of the Czech Republic

32 PUBLICATIONS 115 CITATIONS

[SEE PROFILE](#)

Behavior of Tin-Based “Super-POSS” Incorporated in Different Bonding Situations in Hybrid Epoxy Resins

Adam Strachota,^{*,†} Krzysztof Rodzeń,[†] François Ribot,^{‡,§,||} Miroslava Trchová,[†] Miloš Steinhart,[†] Larisa Starovoytova,[†] and Ewa Pavlova[†]

[†]Institute of Macromolecular Chemistry v.v.i., Academy of Sciences of the Czech Republic, Heyrovského nam. 2, CZ-162 00 Praha, Czech Republic

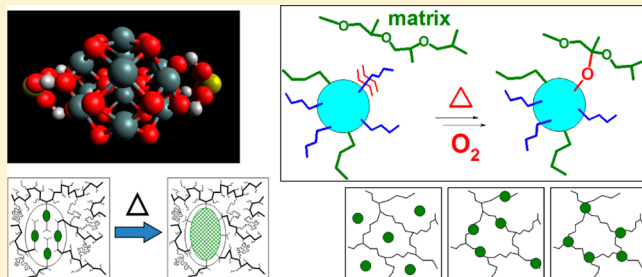
[‡]UPMC Univ Paris 06, UMR 7574, Chimie de la Matière Condensée de Paris, Sorbonne Universités, F-75005 Paris, France

[§]UMR 7574, Chimie de la Matière Condensée de Paris, CNRS, F-75005 Paris, France

^{||}UMR 7574, Chimie de la Matière Condensée de Paris, Collège de France, F-75005 Paris, France

Supporting Information

ABSTRACT: Hybrid organic–inorganic epoxies containing the heavier POSS homologue, *n*-butylstannoxane dodecamer, incorporated as an inert block, as a linear unit, and as a network junction were prepared. This nanometer-sized inorganic cage is especially attractive because of its chemical reactivity (besides mechanical matrix reinforcement). It can undergo oxidative cross-linking reactions with the matrix, or at elevated temperature in the absence of air, it can oligomerize to larger nanodomains, thus generating additional chemical cross-links. The influences of the bonding situation of the stannoxane cages on the hybrid resins’ morphology, mechanical properties, and on the cages’ chemical activity were studied. The highest reactivity was observed in the case of the linearly bonded cages, which also can achieve unusual short-range mobility in the matrix at high temperatures. This mobility was found to be a result of reversible oxonium ionic bonds to the linear units. The branching stannoxane units display a fair antioxidative reactivity in the matrix, which is nevertheless markedly smaller than in the case of the linear ones. On the other hand, the branching cage achieves the highest mechanical reinforcement of the matrix. The nonbonded stannoxane displays macroscopic phase separation at concentrations above 4 wt % and does not reinforce the matrix markedly, but at low concentrations, it is highly efficient in counteracting the oxidative degradation of the matrix. The effect of the stannoxane cages was also systematically compared with the effect of similarly incorporated POSS cages in the same matrix and in general.



1. INTRODUCTION

Tin-based heavy analogues (Scheme 1) of the well-known polyhedral oligomeric silsesquioxane (POSS) cage (Scheme 2) were incorporated into epoxy resins as chemically reactive building blocks with a strong antioxidative effect. The stannoxane cages (“super-POSS”) were incorporated as non-bonding, linearly bonding, and branching structural units. The stannoxane cages and their lighter POSS homologues display sizes close to 1 nm and hence represent large rigid inorganic molecules (molecular SiO_2 or SnO_2). Their dimensions are similar to those of polymer chain segments (“blobs”).^{1,2} From the chemical point of view, such cages are either chemically functionalized (typically 1–12 groups) and incorporated as large classical comonomers (often as branching ones) or—if their surface groups are unreactive—they are dispersed in a polymer matrix similarly like large solvent or plasticizer molecules (polymer blends with “molecular SiO_2 or SnO_2 ”). Although the above hybrid materials are often called “nanocomposites” in the literature, their correct designation is “(organic–inorganic) copolymers” or “blends”, in view of the

inorganic building blocks’ size. In contrast to this, “true nanocomposites” contain a discrete reinforcing nanofiller phase, much larger than polymer chain segments but smaller than 100 nm in at least one dimension. The true nanocomposites already display some internal properties typical for the “macroscopic” composites, while in the above-discussed organic–inorganic copolymers or blends, the key effects are the chemical bonding of the inorganic macromonomers as well as segmental interactions (comonomer–matrix, comonomer–comonomer), topological exclusion by the rigid inorganic structural units, and the inertia of the latter.

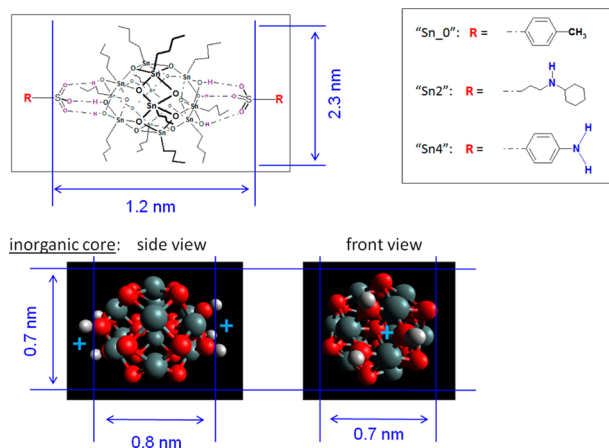
A general advantage of organic–inorganic copolymers, molecular blends, or nanocomposites in comparison with conventional composites consists in the small size of the added inorganic phase, which mostly makes possible the use of the same processing techniques like for the neat matrix.^{3–5} In case

Received: March 9, 2014

Revised: June 9, 2014

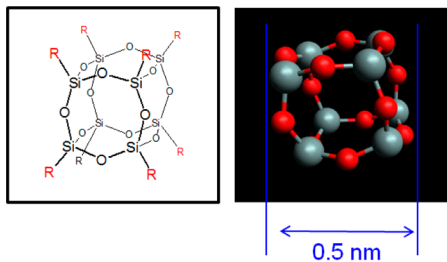
Published: June 23, 2014

Scheme 1. Ellipsoid Butylstannoxane Dodecamer Cage Used in This Work^a



^a $[(n\text{-C}_4\text{H}_9\text{-Sn})_{12}(\text{O})_{14}(\text{OH})_6][\text{O}_3\text{S-(CH}_2)_3\text{-R}]_2$ with different axial end-groups R (bottom left): unreactive toluyl in "Sn_0", mono-amino-H-functional N-cyclohexylaminopropyl in "Sn2" and amino-phenyl in "Sn4".

Scheme 2. Polyhedral Oligomeric Silsesquioxane (POSS) Cage



that the inorganic component's particles are sufficiently small, optical transparency is also preserved. Additionally, the intrinsic properties of the selected inorganic phase can provide specific chemical,^{6–8} optical,^{9–11} electrical,^{12,13} magnetic,^{14,15} or gas barrier^{16–20} properties to the final hybrid material. A marked mechanical reinforcement can be achieved with small amounts of true nanofillers due to their high specific surface.^{21–24}

In their recent work, the authors investigated hybrid epoxy resins reinforced by inorganic POSS cages incorporated as large comonomer and demonstrated the key importance of POSS–POSS interactions for the mechanical reinforcement in these materials.^{25–28}

The tin-based "super-POSS" (oligomeric butylstannoxane cage) shown in Scheme 1 is of interest due to its larger and heavier inorganic core in comparison to POSS and also due to its expected higher chemical reactivity. The latter is connected with the stronger metallic character of Sn and with the weaker Sn–C bond strength. The butylstannoxane dodecamer cage has an 1.2 nm long and 0.7 nm wide ellipsoid (polyhedral) inorganic core, which is covered by substituents, thereby achieving the overall dimensions of approximately 2.3×4.7 nm,²⁹ while the cubic POSS cage (T_8 type) has the dimensions of 0.5 nm (core) and 1.5 nm (core with typical substituents, see Scheme 2). The attachment of two functional (or eventually inert) substituents by ionic bonds in axial positions of the stannoxane ellipsoid is a unique feature of this inorganic

building block, which makes possible its easy incorporation into polymer backbones and into other linear structures.^{38,39}

In contrast to this, POSS can be easily obtained either as a monofunctional or as an octafunctional building block. Ionic dissociation of the stannoxane axial substituents, anion exchange reactions, and supramolecular assembly under specific conditions were reported by Ribot et al.^{30,31} and contribute to this compound's unusual chemistry. A specific property is also the rearrangement into larger structures at elevated temperature (>200 °C), as reported by Ribot et al.²⁹

Well-defined oligomeric alkylstannoxane cages similar to the one shown in Scheme 1 were first prepared in 1989 (POSS already in 1946) by Puff and Reuter,³² followed by Dakternieks.³³ In analogy to siloxane chemistry, a large family of stannoxane compounds exists,^{34–36} including linear, branched, and ladder polymer structures, networks, drums, and cages of different sizes. In 2000, Ribot et al.^{29,37} developed a new, high-yield route (Scheme 4) to the butylstannoxane dodecamer, thus making possible its synthesis on a large scale and its thorough characterization.

To date, only a few pioneering studies have been published concerning polymeric materials containing stannoxane cages: Ribot et al. reported the preparation of carboxylate-based self-assembled organic–inorganic hybrids with stannoxane^{38,39} and a methacrylate–stannoxane copolymer.⁴⁰ Recently, also the authors of this work turned their interest to heavier tin-based POSS analogues and incorporated oligomeric butylstannoxane for the first time into epoxy resins.⁴¹ The stannoxane-modified resins were shown to behave similarly like epoxy-POSS systems but also displayed new properties like the antioxidative action of the inorganic cages at moderately high concentrations (7 wt %). The strong bonding and hence poor extractability⁴¹ of the stannoxane cages were of great importance because of the environmental toxicity of organo-tin compounds. The oligomerization of the cages in the above hybrid resins was also observed at $T > 180$ °C but was found to have little effect on mechanical properties.⁴¹

The aim of this work was to compare the effects of different bonding strategies of the stannoxane cage in an epoxy matrix: Nonbonded (molecularly blended), linearly bonded, and branching stannoxane building blocks (the latter two are comonomers) were studied as to their influence on the hybrid epoxies morphology, mechanical properties, and especially concerning their chemical activity, namely oxidative cross-linking reactions, and stannoxane cage polymerization.

2. EXPERIMENTAL PART

2.1. Materials. The poly(oxypropylene) diamines "Jeffamine D2000" (molecular weight = 1968 g/mol) and "Jeffamine D230" (molecular weight = 230 g/mol), the epoxides diglycidyl ether of Bisphenol A ("DGEBA", 99.7% pure) and phenyl glycidyl ether (PGE), and 1-methylnaphthalene were purchased from Sigma-Aldrich and used as received.

The amino-functional ("Sn2" (MW = 2876.34 g/mol) and "Sn4" (MW = 2780.07 g/mol)) and the nonfunctional ("Sn_0", MW = 2778.10 g/mol) stannoxane cages were synthesized as described in previous work,^{29,37} according to Scheme 4. Butyltin oxide hydroxide hydrate, $\text{BuSnO(OH)} \cdot \text{H}_2\text{O}$, was used as starting material and reacted with toluenesulfonic acid or with sulfanilic acid to yield salts of the stannoxane cage dication shown in Scheme 4, "Sn_0" and "Sn4". The toluenesulfonate was converted into the dihydroxide via an ion exchange reaction using tetramethylammonium hydroxide. The dihydroxide was subsequently neutralized with *N*-cyclohexyl-3-amino-

Table 1. Amounts of Components Used in the Syntheses of the Prepared Hybrid Epoxies

sample name	DGEBA amount [g]	DGEBA amount [mmol]	D2000 amount [g]	D2000 amount [mmol]	Sn cage type	Sn cage [g]	Sn cage [mmol]	toluene added with Sn [g]
matrix	0.127	0.3725	0.367	0.186	none	none	none	none
matrix-pcAr	“_”	“_”	“_”	“_”	“_”	“_”	“_”	“_”
matrix-ox	“_”	“_”	“_”	“_”	“_”	“_”	“_”	“_”
1-Sn_0-n ^a	0.381	1.117	1.100	0.559	Sn_0	0.015	0.005 38	0.015
4-Sn_0-n	0.127	0.3725	0.367	0.186	Sn_0	0.0206	0.007 40	0.020
10-Sn_0-n	0.115	0.337	0.332	0.169	Sn_0	0.0497	0.0178	0.05
24-Sn_0-n	0.097	0.284	0.280	0.142	Sn_0	0.119	0.0428	0.120
24-Sn_0-pcAr	“_”	“_”	“_”	“_”	“_”	“_”	“_”	“_”
24-Sn_0-ox	“_”	“_”	“_”	“_”	“_”	“_”	“_”	“_”
4-Sn2-n	0.120	0.352	0.332	0.169	Sn2	0.0405	0.0141	0.040
10-Sn2-n	0.110	0.323	0.286	0.145	Sn2	0.093	0.0323	0.093
10-Sn2-pcAr	“_”	“_”	“_”	“_”	“_”	“_”	“_”	“_”
10-Sn2-ox	“_”	“_”	“_”	“_”	“_”	“_”	“_”	“_”
25-Sn2-n	0.095	0.279	0.206	0.1045	Sn2	0.200	0.0697	0.200
25-Sn2-pcAr	“_”	“_”	“_”	“_”	“_”	“_”	“_”	“_”
25-Sn2-ox	“_”	“_”	“_”	“_”	“_”	“_”	“_”	“_”
10-Sn4n	0.125	0.367	0.325	0.165	Sn4	0.0510	0.0183	0.051
25-Sn4-n	0.115	0.337	0.249	0.1265	Sn4	0.117	0.0422	0.120
25-Sn4-pcAr	“_”	“_”	“_”	“_”	“_”	“_”	“_”	“_”
25-Sn4-ox	“_”	“_”	“_”	“_”	“_”	“_”	“_”	“_”

^aA large sample, sized 30 × 30 × 1 mm, was prepared in view of the small stannoxane amount to be weighed.

propanesulfonic acid, thus yielding “Sn2”. All the above-mentioned chemicals were purchased from Sigma-Aldrich and used as received.

2.2. Synthesis of the Epoxystannoxane Resins. The organic–inorganic epoxy resins, which were prepared from the DGEBA-D2000 matrix and the stannoxane cages, are listed in Table 4, including the weights and molar amounts of the components used for their synthesis as well as solvent volumes. Only stoichiometric formulations were prepared, the stoichiometry being defined by the molar ratio of functional groups $r = (\text{amino-H})/(\text{epoxy}) = 1$. To each sample in Table 4 an abbreviated name is assigned: The content of amino-functional stannoxanes (“Sn2” and “Sn4”) in the synthesis formulations (as they were mixed) is expressed by the molar percentage of stannoxane amino protons among all amino protons: The abbreviation “25-Sn2” describes an epoxy copolymer in which 25 mol % of amino protons stem from the “Sn2” cage, while the remaining 75 mol % stem from the amino component of the matrix, D2000. In the case of the incorporation (molecular blending) of the nonfunctional cage “Sn_0”, its amount is expressed as wt % in the abbreviated samples names in Table 4: e.g., “24-Sn_0” means 24 wt % of “Sn_0”. The curing conditions are also part of the sample names: The suffix “-n” (e.g., “25-Sn2-n”) describes a normally cured sample and “-pcAr” (e.g., “25-Sn2-pcAr”, see procedure below) means an additional postcure under argon (cage oligomerization, procedure described below), while “-ox” (e.g., “25-Sn2-ox”) means an additional oxidation treatment after the normal cure (procedure described below).

Preparation of Normally Cured Samples. The amounts of the molten and supercooled epoxide DGEBA, of the liquid Jeffamine D2000, and of a 50 wt % stannoxane cage solution in toluene—as listed for each sample in Table 4—were mixed at room temperature in an open 25 mL flask with a magnetic stirrer (the open flask was flushed with argon at the begin of the stirring), and the so-obtained homogeneous clear reaction mixture was heated with an oil bath set at 120 °C and stirred until gelation (typically ca. 40 min). For example, for the synthesis of “10-Sn2-n”, 0.110 g (0.323 mmol) of DGEBA was mixed with 0.286 g (0.145 mmol) of D2000 and with a solution made from 0.093 g (0.0323 mmol) of “Sn2” and 0.093 g of toluene (see Table 4). It was advantageous to prepare larger amounts (e.g., 30 g) of supercooled DGEBA as reserve for the syntheses, by gentle ($\text{mp} = 48$ °C) melting and subsequent cooling to room temperature (DGEBA can stay in the supercooled state for weeks).

When the reaction mixture approached the gel point (the magnetic stirrer just became immobilized), solvent rests were removed by briefly (5 min) applying vacuum at 120 °C, with the help of a Schlenk cap. Thereafter, the plastic (and also clear, homogeneous) early postgel mixture was pressed into a mold, which was put for 3 days into an oven with forced air circulation set at the temperature of 120 °C. The mold consisted of a silicone rubber plate of 1 mm thickness in which an opening sized 30 × 10 × 1 mm (standard sample size) was cut and of two Teflon plates (5 mm thick) which covered the rubber mold from both sides (the cured resins easily separate from Teflon). The mold assembly was pressed together by two steel plates (5 mm thick) fixed by screws. There was no channel connecting the sample volume in the rubber mold with the surrounding environment, so that no air was entering the mold during the normal cure. In the case of the sample “1-Sn_0-n” (see Table 4), a rubber mold with a larger opening sized 30 × 30 × 1 mm was used (in order to reach reasonably weighable stannoxane amounts during synthesis). Up to six specimens of each hybrid resin were typically prepared (in separate glasses): one for characterization after normal cure, one for characterization after annealing under argon, one for characterization after oxidation treatment, and three more for extraction experiments (after the respective cure or treatment).

Stannoxane Cage Oligomerization via Additional Postcure (Annealing) under Argon. Postcure (after normal cure) of the prepared hybrid resins was achieved in the following way: the respective sample (size 30 × 10 × 1 mm) was put into a wide-neck glass ampule filled with argon, which was subsequently sealed using a gas burner. The sample in the ampule was put for 12 h into an oven with forced air circulation set at the temperature of 180 °C. Thereafter, the sample in the ampule was cooled down to room temperature, the ampule was broken, and the sample was stored.

Oxidation treatment of the prepared hybrid resins was performed (after normal cure) by heating unprotected samples for 12 h in an oven with forced air circulation, set at 180 °C. The sample size was always identical: 30 mm height, 10 mm width, and 1 mm thickness. A small hole was drilled in the top of each sample, and the samples were hanging on a thin wire in the central part of the oven, in order to ensure an optimal access of the circulating air. In the case that several samples were subjected to the oxidation treatment simultaneously, they were separated by ceramic Raschig rings in order to achieve distances about 3 cm.

Table 2. Components Amounts in Reaction Mixtures Used for Reactivity Assessment of Amino Compounds

experiment	toluene (solvent) [g]	PGE amount [g]	PGE amount [mmol]	1-MeNph amount (standard) [g]	1-MeNph amount (standard) [mmol]	amine amount [g]	amine amount [mmol]
"Sn4" reactivity	3.15	0.770	5.13	0.219	1.538	0.891	0.320
"Sn2" reactivity	2.39	0.709	4.72	0.201	1.416	1.697	0.590
"D230" reactivity	3.86	0.826	5.50	0.235	1.650	0.079	0.344

Epoxy-POSS copolymers used for comparative tests were prepared according to the authors' previous work^{25,26} and were subsequently subjected to the same above-described annealing and oxidation treatments like the epoxystannoxane resins.

2.3. Reactivity Investigation. The reactivity of the amino-functional stannoxyanes "Sn2" and "Sn4" toward epoxides was compared with the reactivity of Jeffamine D230 (poly-(oxypropylene)- α,ω -diamine), a low-molecular-weight analogue of the amino component in the studied hybrid epoxies (D2000). The monofunctional phenyl glycidyl ether (PGE) was used as epoxy reactant in these tests because of its high chemical similarity to DGEBA. The experiments were carried out at 4-fold epoxide excess; the starting concentrations of epoxy groups were 1 mol/L and those of amino groups 0.25 mol/L.

Preparation of Kinetics Samples. Toluene (solvent), PGE, 1-methylnaphthalene (integration standard, 1-MeNph:PGE ratio was 0.3), and the tested amine ("Sn4" or "Sn2" or D230) were mixed in the amounts given in Table 2 for each reactivity investigation. Each reaction mixture was briefly stirred and divided into 10 small glass ampules filled with argon, which were sealed with a gas burner. Each ampule was immersed into an oil bath set at 120 °C in order to reach a desired reaction time at this temperature (20 min, 40 min, 1 h, 2 h, 1 day, 2 days, and 3 days). Thereafter, the "ampule samples" were "quenched" with liquid nitrogen and stored in a freezing box at -35 °C. Just before the analysis of the conversion degree via ¹H NMR, the samples were dissolved in CDCl₃. (The investigated reactions proceed very slowly at room temperature and stand still in the time scale of weeks at -35 °C.)

Evaluation of the Reaction Rate of the Epoxide–Amine Addition via ¹H NMR Spectroscopy. In Figure 1, a typical ¹H NMR spectrum of

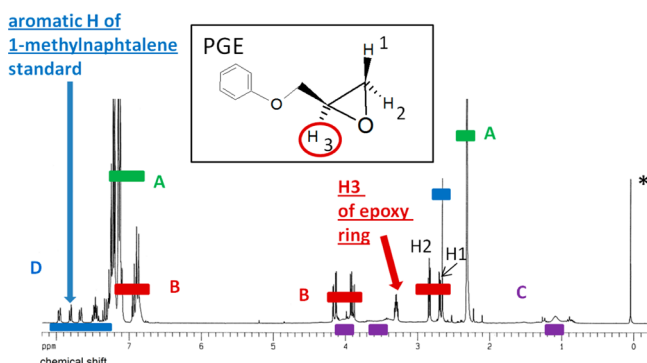


Figure 1. ¹H NMR signals used for the determination of the epoxy group conversion. Assignment: toluene (solvent) signals (A), signals of phenyl glycidyl ether (B), signals of the tested amino component, Jeffamine D230 in the given example (C) and 1-methylnaphthalene (integration standard, D).

an investigated epoxide–amine reaction mixture is shown, on the example of the reaction of the Jeffamine D230 with PGE. The concentration of the epoxy groups was determined by following the relative intensity (ratio (signal integral/standard signal integral)) of the oxirane ring H signal near 3.32 ppm (see "H3" in Figure 1), which was always well-separated from all the other signals of starting compounds and of products. As internal integration standard, the nonvolatile 1-methylnaphthalene was used, namely the integral of its

well-separated aromatic signal at 7.81 ppm. The above-mentioned integrals of the oxirane and of standard signals in dependence of reaction time for all the three investigated reactions, Sn4 + PGE, Sn2 + PGE, and D230 + PGE, are given in Table 3.

Table 3. Integrals of the Characteristic Signals of the Oxirane Rings and of the 1-Methylnaphthalene Standard in Dependence of the Reaction Time Endured at 120 °C as Well as the Calculated Relative Content of Epoxy Groups in the Reaction Mixtures D230 + PGE, Sn2 + PGE, and Sn4 + PGE

Jeffamine D230 + PGE						
time [min]	0	20	60	120	1440	2880
MeNph at 7.81 ppm	1.00	1.00	1.00	1.00	1.00	1.00
PGE at 3.32 ppm	3.07	3.00	2.88	2.83	2.56	2.45
Ep groups [%]	100	97.6	93.9	92.1	83.2	79.8
"Sn2" + PGE						
time [min]	0	20	40	120		
MeNph at 7.81 ppm	1.00	1.00	1.00	1.00		
PGE at 3.32 ppm	3.08	2.47	2.14	1.88		
Ep groups [%]	100	80.3	69.5	61.2		
"Sn4" + PGE						
time [min]	0	20	60	120	408	805
MeNph at 7.81 ppm	1.00	1.00	1.00	1.00	1.00	1.00
PGE at 3.32 ppm	3.03	3.02	3.005	2.98	2.88	2.77
Ep groups [%]	100	99.7	99.0	98.1	94.9	91.4

The chemical shifts (δ) of the ¹H NMR signals observed in the kinetics spectra, most of which can be seen in Figure 1, are assigned as follows: Toluene (solvent): marked with "A" and with green color in Figure 1: 7.2–7.1 ppm (aromatic H), 2.34 ppm (methyl group); 1-methylnaphthalene (internal integration standard): marked with blue color and "D" in Figure 1: 7.96, 7.81, 7.67, 7.45 and 7.48, 7.33, and 7.28 ppm (aromatic H), 2.65 ppm (methyl); PGE: marked with red color and "B" in Figure 1: 7.1–6.8 ppm (aromatic H), 4.17 and 3.94 ppm (Ep-CH₂-O-), 3.32 ppm (oxirane-H3), 2.85 ppm (oxirane H2), 2.72 ppm (oxirane-H1); D230: marked with violet color and "C" in Figure 1: 4.00 ppm (-O-CH₂-), 3.50 ppm (-CH₂-O-), 1.12 ppm (methyl); "Sn4" (not shown in Figure 1): 7.66 and 7.62 ppm (aromatic H in the axial substituents), 7.02 ppm (OH groups of the stannoxyane cage), 3.84 ppm (NH₂ groups), 1.85–1.25 ppm (CH₂ groups in *n*-butyl substituents), 0.95 and 0.89 ppm (CH₃ groups in *n*-butyl substituents); "Sn2" (not shown in Figure 1): 2.89 ppm (-CH₂-SO₃), 2.75 ppm (-CH₂-NH- in axial substituents), 2.43 ppm (>CH-NH- in the cyclohexyl groups), 2.00 (CH₂ in the cyclohexyl groups), 1.89 ppm (C-CH₂-C in axial substituents), 1.85–1.25 ppm (CH₂ groups in *n*-butyl substituents and cyclohexyl groups), 0.95 and 0.89 ppm (CH₃ groups in *n*-butyl substituents).

Determination of Times of Gelation of Reaction Mixtures with "Sn_0". The same amounts of the molten and supercooled epoxide DGEBA, of the liquid Jeffamine D2000, and of a 50 wt % "Sn_0" cage solution in toluene, as listed in Table 4 for samples "1-Sn_0-n" until

"24-Sn_0-n", were mixed at room temperature in argon-filled 10 mL glass ampules which contained magnetic stirrers. Thereafter, the ampules were sealed with a gas burner. Each ampule was subsequently immersed into an oil bath set at 120 °C, and the reaction mixture was stirred with the magnetic stirrer. The approximate time of gelation was observed as the time after which the magnetic stirrer became immobilized by the reaction mixture.

¹H and ¹¹⁹Sn NMR Spectroscopy. ¹H and ¹¹⁹Sn NMR spectra were recorded on a Bruker (Karlsruhe, Germany) Avance DPX 300 spectrometer at 300 MHz (¹H NMR) and at 111.92 MHz (¹¹⁹Sn NMR). The ¹¹⁹Sn {¹H} spectra were obtained with a composite pulse decoupling sequence (CPD). CDCl₃ was used as solvent for all experiments (¹H and ¹¹⁹Sn). The ¹¹⁹Sn chemical shifts are quoted relatively to the tetramethyltin standard ($\delta = 0$ ppm), in whose place the nonvolatile tetrabutyltin was used ($\delta = -7$ ppm).

FT-IR Investigation of Stannoxane Cage Polymerization. Fourier transform infrared spectroscopy investigations (FT-IR) were performed in an attenuated total reflection (ATR) mode using a Thermo Nicolet NEXUS 870 FTIR spectrometer (Madison, WI). Spectra of the powdered samples were measured with Golden GateTM Heated Diamond ATR Top-Plate (MKII single reflection ATR system; Specac; Orpington, UK).

2.4. Characterization of the Epoxystannoxane Resins. TEM. Transmission electron microscopy (TEM) was performed using the Tecnai G2 Spirit Twin 12 microscope (FEI, Czech Republic) after preparing ultrathin sections (approximately 60 nm thick) from the originally synthesized hybrid resin platelets by an ultramicrotome (Ultracut UCT, Leica, Germany) under cryogenic conditions (the sample and knife temperatures were -80 and -50 °C, respectively). Each specimen section was transferred to a microscopic grid and observed in the bright field mode at the acceleration voltage of 120 kV.

SAXS. Epoxystannoxane resin samples were characterized by SAXS as obtained from the mold (rectangular platelets sized 30 × 10 × 1 mm) and were fixed with Scotch tape on a steel multisample holder with circular windows (5 mm diameters). SAXS profiles of the neat stannoxane cages were measured by fixing finely powdered crystals on Scotch tape, the SAXS profile of which was subsequently subtracted from the result.

SAXS experiments were performed using a pinhole camera (Molecular Metrology SAXS System) attached to a microfocused X-ray beam generator (Osmic MicroMax 002) operating at 45 kV and 0.66 mA (30 W). The camera was equipped with a multiwire gas-filled area detector with an active area diameter of 20 cm (Gabriel design). Two experimental setups were used to cover the q range of 0.005–4 Å⁻¹. The scattering vector, q , is defined as $q = (4\pi/\lambda)\sin \theta$, where λ is the wavelength and 2θ is the scattering angle. The scattering intensities were put on an absolute scale using a glassy carbon standard. Calibration of primary beam position and sample-to-detector distances was performed using a silver behenate sample.

Fraction of Gel and Stannoxane Cage Extraction. Gel Fraction of the Entire Hybrid Resin. The extraction analysis of the prepared epoxystannoxane resins was carried out as follows: The samples were swollen and extracted with toluene/THF (1:1). All the samples were extracted for 3 days while the solvent was changed every day for a pure charge. After the extraction, the samples were dried (vacuum, 100 °C) until weight constancy and the fraction of gel (w_g) was determined as

$$w_g = \text{mass (dry, after extraction)} / \text{mass (dry, before extraction)}$$

The stannoxane cage extraction (via SnO₂ ash analysis) was determined as follows: The tested sample (standard rectangular sample: 30 × 10 × 1 mm, weight ca. 360 mg) was divided into two pieces. Only one of these pieces (180 mg) was subjected to the above extraction. Both samples (180 mg) were subsequently subjected to ash analysis. Dividing the ash content of the extracted sample piece by the ash content of the nonextracted one directly yields the gel fraction of the cage. The ash content for this calculation was expressed in %, relative to the original sample weight. The ash analyses were performed as follows: The hybrid resin samples (ca. 180 mg) were first weighed and thereafter put into a platinum pot together with the double of their weight of sulfuric acid (360 mg). This mixture was

slowly pyrolyzed in air (heating at around 337 °C, the boiling point of H₂SO₄). The remaining ash was heated to ca. 1000 °C for 15 min. The pyrolysis with the sulfuric acid was repeated once more with the ash. The dry SnO₂ ash was then weighed.

The fraction of gel for the matrix alone was calculated from the gel fraction of the entire composite, from the gel fraction of the stannoxane cage and from the original (at synthesis) cage content as follows:

$$w(m) = (1/(1-R))w(g) - (R/(1-R))w(f)$$

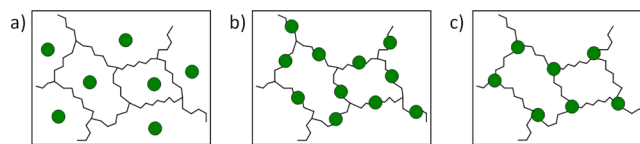
where $w(m)$ = gel fraction of the matrix alone, $w(g)$ = overall fraction of the entire composite, $w(f)$ = gel fraction of cages, and R = original cages amount ($= m(\text{cages})/m(\text{all})$).

DMTA. Dynamic mechanical properties of the epoxystannoxane resins were tested with rectangular platelet samples as obtained from the mold, sized 30 × 10 × 1 mm, using an ARES G2 apparatus from TA Instruments. An oscillatory shear deformation (0.1%) at the constant frequency of 1 Hz and at the heating rate of 3 °C/min was applied, and the temperature dependences of the storage shear modulus and of the loss factor (G' and $\tan(\delta)$, respectively) were recorded. The temperature range was typically from -100 to +120 °C (or -100 to +100 °C in the case of samples that were not postcured; in some cases the DMTA was recorded up to +150 °C).

3. RESULTS AND DISCUSSION

The goal of this work was the preparation of hybrid epoxy resins with nonbonded, linearly bonded, and branching butylstannoxane dodecamer cages (see Scheme 3) and the

Scheme 3. Incorporation of (a) Nonbonded, (b) Linearly Bonded, and (c) Branching Stannoxane Cages into an Epoxy Matrix

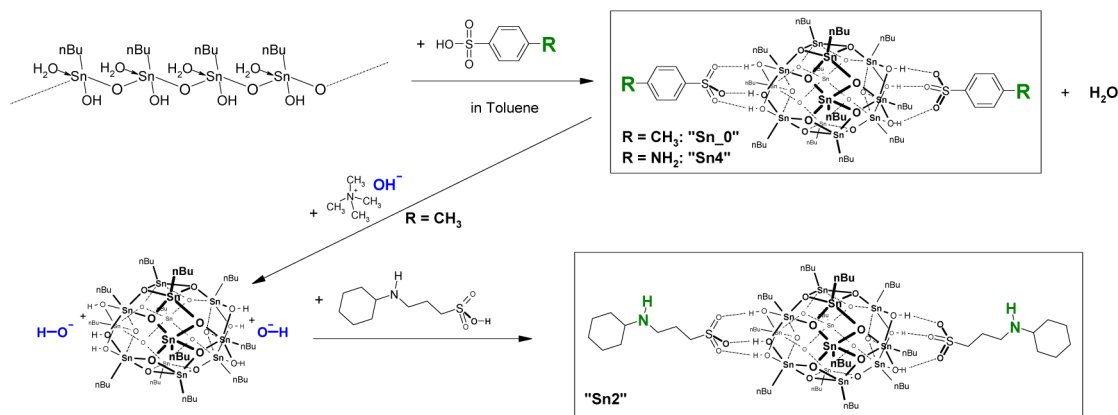


subsequent comparison of the effects of these inorganic cages in the different situations. As mentioned in the Introduction, the studied hybrid resins are properly described as copolymers or blends (nonbonded stannoxane) because the inorganic building block has the size of a large molecule, while in a part of the literature, similar systems are controversially called nanocomposites. The stannoxane cage can be considered as a heavier homologue of the well-known POSS cage (of similar size), but its distinct feature is its chemical reactivity: the oxidative cross-linking reactions with suitable matrices as well as oligomerization at temperatures above 200 °C.

In the following sections, we discuss the synthesis of nonbonding, linearly bonding, and branching stannoxane cages, their reactivity and ability to disperse in epoxy matrices, and their effects on thermomechanical properties. Furthermore, the oligomerization was studied in some detail, especially its chemistry (¹H and ¹¹⁹Sn NMR, FT-IR spectroscopy) and also its consequences for the morphology and for the mechanical properties of the studied three types of epoxystannoxane resins. Finally, the ability of the three cage types to counteract the oxidative degradation of the epoxy matrix by undergoing cross-linking with the latter was compared. Minimal stannoxane cage concentrations necessary for efficient matrix protection were determined.

3.1. Synthesis of the Heavier POSS Analogue. The organo-tin-oxo cages are synthesized similarly like their lighter

Scheme 4. Synthesis of the *n*-Butylstannoxane Dodecamer Cages with Tolyl (“Sn_0”), *N*-Cyclohexylaminopropyl (“Sn2”), and Aminophenyl (“Sn4”) End Groups



POSS homologues via the sol–gel process of the compounds R-E(OH)₃, (E = Si or Sn, R = organyl). Some R-Sn(OH)₃ compounds are commercially available in the partly condensed form [R-Sn(O)OH]_n and can be used as starting materials for catalyzed condensations and rearrangements to oligomeric stannoxane cages or to other stannoxane structures mentioned in the Introduction. Stannoxane dodecamer cages like the ones studied in this work are most easily obtained with *n*-butyl substituents,²⁹ by acid-catalyzed condensation and rearrangement of [nBu-Sn(O)OH]_n as shown in Scheme 4, first step. The cage has an ellipsoid shape, and two sulfonate substituents are attached in axial positions. They stem from the acid used to catalyze the reaction and can be used to introduce functional groups.

The three stannoxane cages studied in this work—the nonbonding “Sn₀”, the linearly bonding “Sn2”, and the branching “Sn4” (incorporated as epoxy network junction)—are shown in Scheme 5. The compounds were obtained by the route of Ribot et al.^{29,37} (Scheme 4), in one (Sn₀ and Sn4) or in three steps (Sn2). The shorter path is only possible if the acid which is to be introduced as an anionic substituent is sufficiently strong but not too aggressive. Some of the more problematic substituents nevertheless can be introduced via the

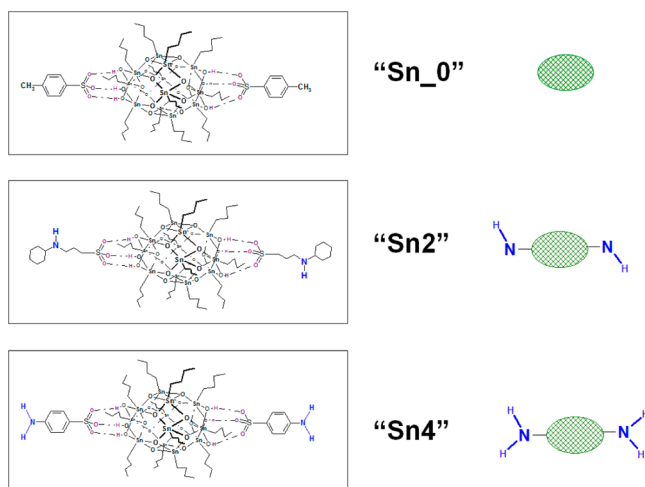
longer path shown in (Scheme 4): Sn₀ is synthesized in the first step, and its axial anionic substituents are exchanged for hydroxide ions, in the polar and protic isopropanol. Subsequently, the hydroxide “end groups” are neutralized by a weak acid (or by a diluted aggressive acid like H₂SO₄).

In this way, a number of stannoxane dodecamer derivatives have been synthesized by Ribot et al., with ionic substituents like carboxylate,^{38,39} diphenylphosphinate,⁴² or oxalate³¹ and also sulfate.³¹ The longer synthesis path fails, however, if an acid is too weak, like an amino acid (e.g., aminosulfonic, aminocarboxylic) with a sufficiently basic amino group. The *N*-cyclohexyl-3-aminopropanesulfonic acid used for the synthesis of Sn2 is close to the limit of synthetic possibilities, while the related sterically unhindered 3-aminopropanesulfonic acid cannot be introduced as ionic substituent by the above route. The relatively high basicity of the *N*-cyclohexyl-3-amino-propanesulfonate anion may play a role in the below-discussed high reactivity of Sn2 as well as in its short-range mobility at high temperatures in spite of chemical incorporation in the copolymeric epoxy resins.

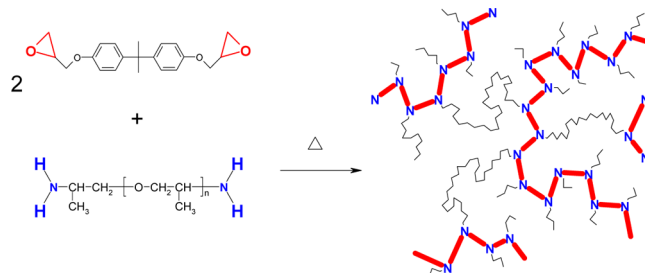
3.2. Stannoxane Cage Dispersion in the Epoxy Matrix.

3.2.1. Synthesis of the Hybrid Epoxy Resins. The epoxy resin, which was modified to obtain organic–inorganic epoxies in this work, was prepared according to Scheme 6. It is based on poly(oxypropylene)- α,ω -diamine (“D2000”, MW = 1968 g/mol) and diglycidyl ether of bisphenol A (DGEBA). This elastomeric matrix was chosen because of its expected high

Scheme 5. Stannoxane Cages Compared in This Work: Nonbonding “Sn₀”, Linearly Bonding “Sn2”, and Branching “Sn4”



Scheme 6. Synthesis of the Polymer Matrix from Diglycidyl Ether of Bisphenol A (DGEBA) and Poly(oxypropylene)- α,ω -diamine “Jeffamine D2000” (34-mer)^a

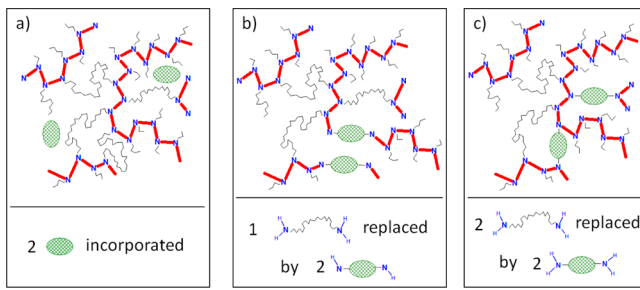


^aIn the matrix structure, DGEBA forms the more rigid chains (red, bold lines) interconnected by long elastic chains of D2000 (black thin lines) at the end of each DGEBA repeat unit.

sensitivity to reinforcing and to chemical effects of incorporated inorganic building blocks: Because of the extended elastic chains, a distinct modulus increase in the rubber plateau should occur in response to additional physical cross-linking (e.g., via stannoxane–matrix, or stannoxane–stannoxane interactions), and the glass transition temperature should be sensitive to topological constraints or to the inertia of the attached large inorganic cages. The long polyoxypropylene chains also contain numerous $\text{CH}-\text{O}-$ groups which can relatively easily undergo radical reactions (e.g., under oxidative conditions). The matrix structure consists of rather rigid chains made of aromatic DGEBA units and of N atoms from D2000, which are interconnected by elastic poly(propylene oxide) chains. The latter connect the N atoms of the “rigid” chains. The resin was cured in a hermetic rectangular mold ($30 \times 10 \times 1$ mm) in the absence of air at 120°C for 3 days (referred to as “standard cure conditions”).

The organic–inorganic resins prepared from the DGEBA-D2000 system and Sn₀, Sn2, and Sn4 cages are shown in Scheme 7. Resins modified with Sn₀ were obtained by

Scheme 7. Idealized Structures of the Hybrid Epoxies Based on the DGEBA-D2000 Matrix and the “Sn₀”, “Sn2”, and “Sn4” Cages



blending Sn₀ with the matrix components prior to cure. In the epoxy-Sn4 hybrids (copolymers), the branching Sn4 (amino-H-tetrafunctional) is introduced as replacement of a part of the branching and elastic D2000 (amino-H-tetrafunctional; structure: two junctions connected by a spring). The cross-link density theoretically should not decrease, but the matrix becomes more rigid. Finally, the epoxy-Sn2 copolymers were obtained by replacing a part of D2000 by “Sn2” (amino-H-bifunctional, linear units). This causes a decrease of chemical cross-link density, although under favorable conditions, some

Sn2 units should form physical cross-links via Sn2–Sn2 interactions (see Scheme 7b).

The syntheses of the hybrid epoxies were performed similarly like the neat matrix synthesis: the appropriate amounts of liquid D2000, supercooled liquid DGEBA, and of a 50 wt % solution of the respective stannoxane cage (see Table 1, Experimental Part) in toluene were mixed and stirred under argon at 120°C until gelation. Thereafter, the solvent was removed under vacuum, and the plastic early postgel mixture was pressed into a mold (rectangular shape, $30 \times 10 \times 1$ mm) and cured in the absence of air at 120°C for 3 days (“standard cure”). The use of solvent was necessary to ensure a fine cage dispersion at higher stannoxane loadings. The solvent was used also with small stannoxane amounts to simplify mixing with the matrix components.

3.2.2. Reactivity of the Stannoxane Cages. In order to qualitatively evaluate the process of stannoxane cages incorporation into the epoxy resin, the reactivity of the amino-functional stannoxanes Sn2 and Sn4 was investigated and compared with the reactivity of poly(oxypropylene)- α,ω -diamine D230, a lower molecular weight analogue of D2000 (see Figure 2): The amino compounds Sn2, Sn4, and D230 were reacted with a model epoxide, phenyl glycidyl ether (chemically very similar to DGEBA), and their rates of conversion were compared. ¹H NMR spectroscopy was employed, and the integral of the epoxy group signal at 3.30 ppm was used to determine the epoxy group concentration. It was preliminarily assumed that the epoxy groups disappear only via addition reactions with amino groups, i.e., that the ring-opening polymerization of the epoxy groups does not play a dominant role under the test conditions.

The reactivity comparison in Figure 2 implies that Sn2 reacts much faster with DGEBA than D2000, thus being incorporated preferentially in the early reaction stages (see Scheme 8). This effect is expected to favor the fine dispersion of Sn2 in epoxy copolymers. It also can be noted (Figure 2) that the stannoxane Sn2 (in contrast to Sn4 or D230) catalyzes the epoxy groups ring-opening polymerization (ROP), so that the epoxy concentration decreases below the theoretical limit. It seems nevertheless that the ROP reaction is not dominant and that it is markedly slower than the desired epoxide–amine addition: In Figure 2, the decrease of the epoxy groups’ concentration considerably slows down after the consumption of all the amino protons (theoretically 25% conversion of epoxy groups). Most of the originally available epoxy groups (ca. 70%) remain available for the competing ROP reaction at this point, but they

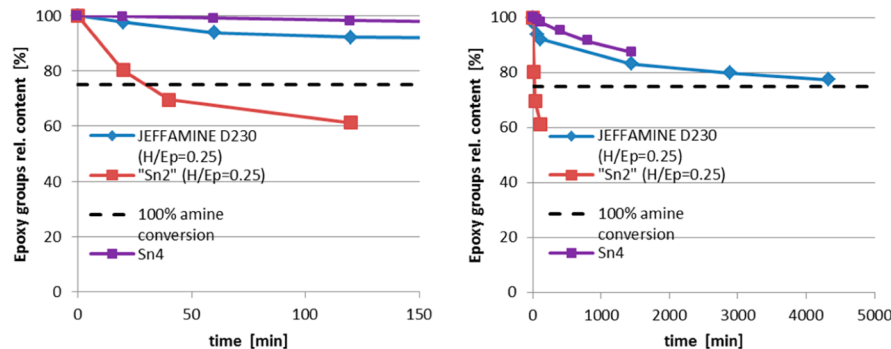
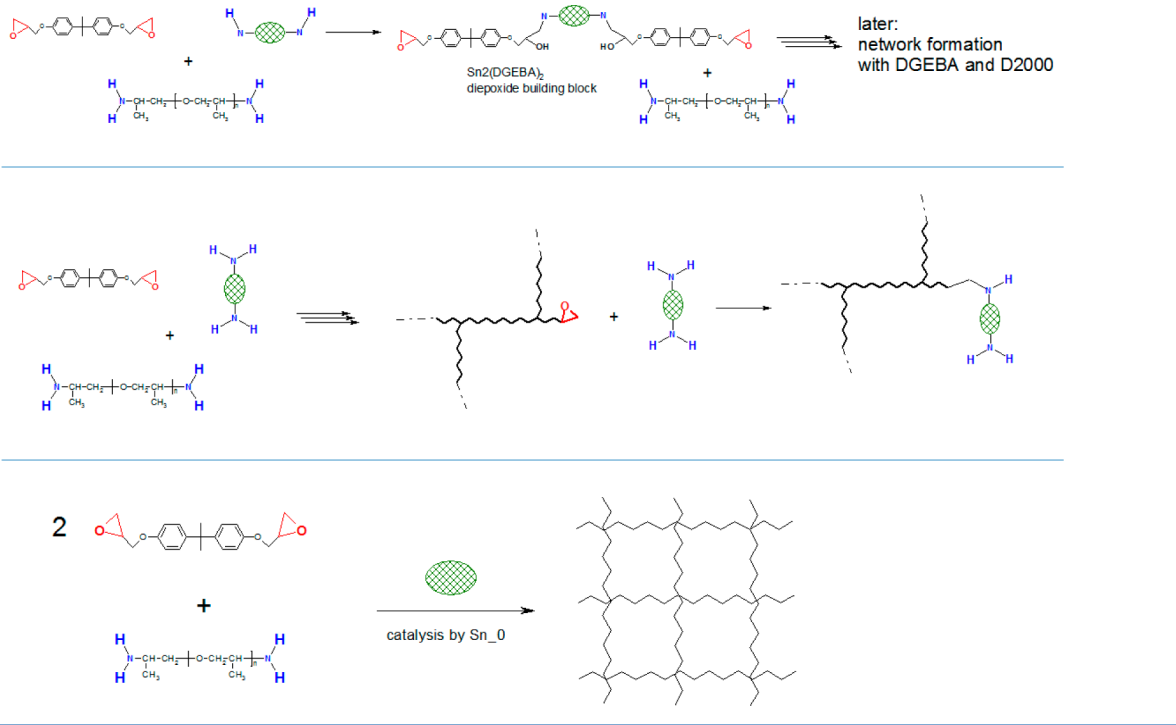


Figure 2. Relative reactivity: kinetic curves of consumption of epoxy functions of phenyl glycidyl ether in reaction with the amino-functionalized cages “Sn2” and “Sn4” and with Jeffamine D230, a low molecular weight analogue of the amino component of the matrix. $T = 120^\circ\text{C}$, in sealed ampule, $r(\text{H}(-\text{N})/\text{Ep}) = 0.25$, $c_0(\text{Ep}) = 1 \text{ M}$, $c_0(\text{Am}) = 0.25 \text{ M}$; in toluene, epoxy groups are assumed to disappear by reaction with amine.

Scheme 8. Chemical Behavior of Sn₂, Sn₄, and Sn_0 Cages during the Synthesis of the Organic–Inorganic Epoxy Resins

react relatively slowly in comparison with the preceding addition reaction with amine. Also, the below-discussed mechanical properties of the epoxy-Sn₂ resins seem to indicate that the eventual ROP side reaction does not have a marked influence on the hybrid epoxies. The high reactivity of Sn₂ (in addition and ROP reactions) is probably connected with the easily dissociating oxonium bond to the axial substituents, which will be discussed below.

In contrast to Sn₂, the Sn₄ cage with aromatic amine groups displays a lower reactivity toward epoxies than D2000, as determined in earlier work.⁴¹ This leads to the preferential reaction of DGEBA with D2000 in the earlier stages of the epoxy copolymer formation, while Sn₄ is incorporated in the later stages (Scheme 8). This favors a nanophase segregation of Sn₄, which was discussed in previous work.⁴¹ The reactivity of Sn₄ is nevertheless higher than theoretically expected,⁴¹ most likely due to a catalytic effect of the oxonium ionic bonds carrying the axial substituents.

Interestingly, the Sn₀ cage, which is not chemically bonded to the epoxy matrix, also influences its formation chemistry: it catalyzes the epoxy resin cure (Scheme 8), as illustrated by decreasing times of gelation of the reaction mixture with increasing amounts of added Sn₀ (Figure 3). The oxonium bonds to the axial substituents of Sn₀ are most likely responsible for this effect. The mechanism suggested by the authors is the partial (Scheme 9) or full (Scheme 13) dissociation of the oxonium bond, followed by the protonation (eventually only via H-bridging) of the oxirane O atom by the sulfonic acid OH group (Scheme 9), thus yielding an activated epoxide. This hypothetical mechanism is supported by FTIR spectroscopic investigation of the oxonium bonds in Sn₀, Sn₂, and Sn₄ at temperatures up to 120 °C (see discussion of stannoxane oligomerization below).

3.2.3. Morphology of the Epoxystannoxane Resins after Standard Cure. The dispersion of the cages Sn₀, Sn₂, and Sn₄ in the DGEBA-D2000 matrix was studied by transmission

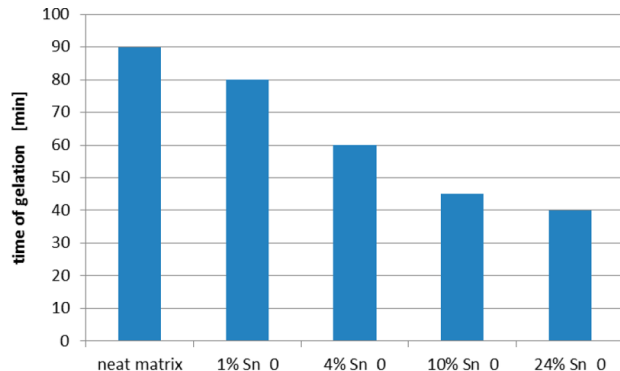


Figure 3. Catalytic effect of the nonbonding cage “Sn₀” on the epoxide–amine addition (matrix formation reaction), observed with decreasing times of gelation of the reaction mixtures used to prepare the neat matrix and the organic–inorganic resins with 1–24 wt % Sn₀.

electron microscopy (TEM) and by X-ray scattering (SAXS + WAXS). A strong tendency for Sn₀ phase separation and crystallization (WAXS) was clearly observed, but at 1 wt %, a homogeneous Sn₀ dispersion was achieved. Sn₂ and Sn₄ disperse homogeneously.

TEM. The TEM investigations illustrate the difference in morphology between the blend-type resins with Sn₀ on one hand and the copolymer-type ones containing Sn₂ and Sn₄ on the other.

Epoxy-Sn₀ hybrids (blends) can be obtained as highly homogeneous materials only at the lowest stannoxane loads, 1 wt % or lower (see Figure 4). At 4 wt %, occasional Sn₀ nanodomains appear, while at 10 wt % some of the heterogeneities reach submicrometer dimensions. Finally, at 24 wt %, micrometer Sn₀ crystallites can be observed (see Supporting Information Figure 1). The phase separation of

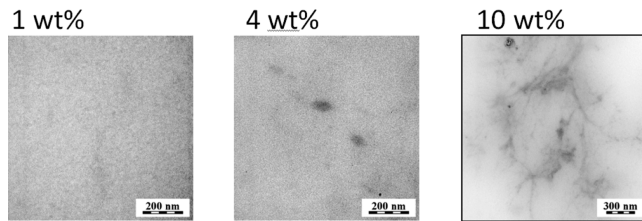
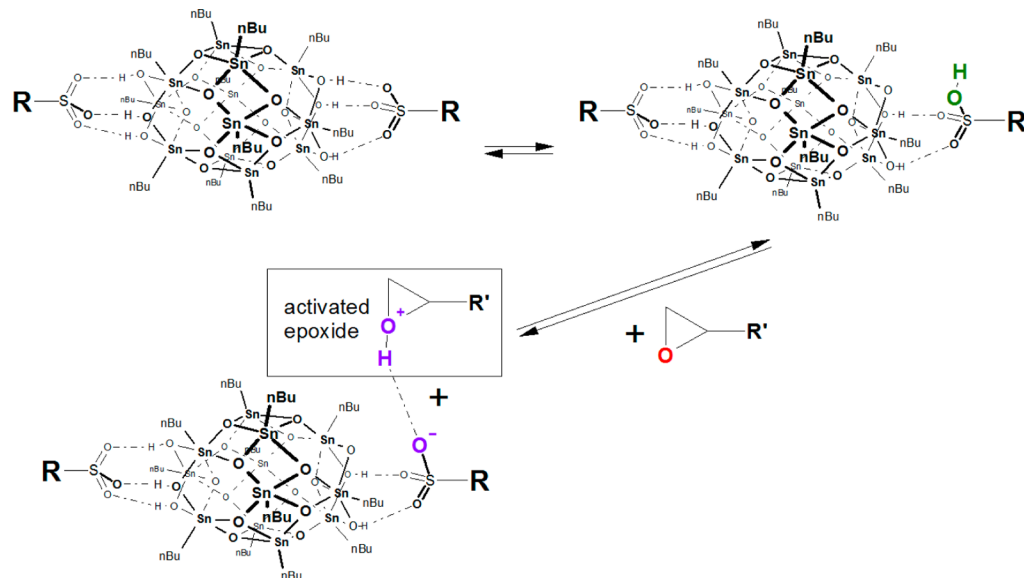
Scheme 9. Tentative Mechanism of the Catalytic Effect of “Sn_0” on the Epoxide–Amine Addition

Figure 4. Transmission electron microscopy (TEM) images of the epoxy-Sn₀ resins based on DGEBA-D2000 and containing 1–10 wt % Sn₀; the samples underwent standard cure at 120 °C.

Sn₀ is a logical consequence of the absence of bonds to the matrix (no reaction blending).

The Sn₂ and Sn₄ copolymers with DGEBA-D2000 are practically homogeneous at all concentrations (see examples in Supporting Information Figure 2). For Sn₂, some occasional inhomogeneity can be observed at high Sn₂ loads (e.g., at 50 mol % ≡ 63 wt %, Supporting Information Figure 2b).

X-ray Scattering (SAXS + WAXS). The phase structure of the hybrid resins with the Sn₀, Sn₂, and Sn₄ cages was further studied by means of X-ray scattering (SAXS + WAXS). The results are illustrated in Figure 5. The scattering patterns confirm the highly homogeneous morphology of the copolymer-type resins containing Sn₄ and Sn₂: Only very small aggregates of few cages are observed at high cage contents. The crystallization of Sn₀ above 1 wt % was also clearly confirmed by X-ray scattering.

The scattering patterns of the studied organic–inorganic hybrid resins can be divided into four characteristic regions:

At high values of the scattering vector q (high scattering angles, region (1) in Figure 5, top), between $q = 1.1$ and 2.8 \AA^{-1} , which correspond to characteristic distances of 0.55 – 0.2 nm , interferences are observed corresponding to typical intermolecular distances of hydrocarbon chains (“amorphous halo”). These interferences are observed in the neat matrix (e.g., distances of neighboring D2000 chain segments), in the hybrid resins, and in the neat stannoxane cages, where they can be assigned to intramolecular distances of the butyl substituents in the organic shells of the cages.

The second characteristic region, also at high scattering vectors, between q values of 0.2 and 0.8 \AA^{-1} (characteristic distances of 2.5 – 0.75 nm , region (2) in Figure 5, top), can be clearly assigned to intramolecular interferences on the inorganic cores of the stannoxane cages (including the SO₃ groups and phenyl rings attached to them, compare Scheme 1). The group of the stannoxanes’ intramolecular interference signals does not change its position with cage dilution. The neat Sn₂ cage does not display the interference peak near $q = 0.25 \text{ \AA}^{-1}$ (distance 2.5 nm); its lowest- q intramolecular interference is observed at $q = 0.44 \text{ \AA}^{-1}$ (distance 1.4 nm), which corresponds to the inorganic core with SO₃ groups (compare Scheme 1). For all the studied stannoxane cages, neat as well as in the hybrid resins, the maximum of the interference peaks group is found near $q = 0.49 \text{ \AA}^{-1}$ (distance 1.3 nm). The resins blended with Sn₀ display sharp peaks, characteristic of crystallites, in this region, if the Sn₀ concentration is 4 wt % or higher: At 1 wt % no crystalline peaks are observed; at 4 and 10 wt % a small but increasing intensity of the crystallite peaks is observed. At 24 wt %, the crystallite signals are the dominant feature of the whole WAXS + SAXS pattern, which is very similar to that of neat Sn₀. The observations correspond very well with the TEM images of the epoxy-Sn₀ resins.

In the third characteristic region, between $q = 0.04$ and 0.3 \AA^{-1} (region (3) in Figure 5, top), two characteristic features can be observed: A broad interference maximum of the neat matrix DGEBA-D2000 is centered near 0.15 \AA^{-1} (visible also in hybrid resins with a low stannoxane loading, e.g., 1 wt % Sn₀), which corresponds to the distance of 4.2 nm and which can be assigned to coiled poly(propylene oxide) chains of D2000. Second, the resins with well-dispersed stannoxane cages and with a cage content above 20 wt % display a step in scattering intensity near 0.1 \AA^{-1} (distances 4 – 10 nm), covering the “D2000 peak”, which might be assigned to small aggregates composed of a few stannoxane cages (not visible in the above TEM images). The scattering step hence can be correlated with the stannoxane-rich phase whose relaxation can be observed via dynamic mechanical thermal analysis (DMTA) (see below).

In the region of very low scattering vector values, between $q = 0.005$ and 0.04 \AA^{-1} (region (4) in Figure 5, top), the

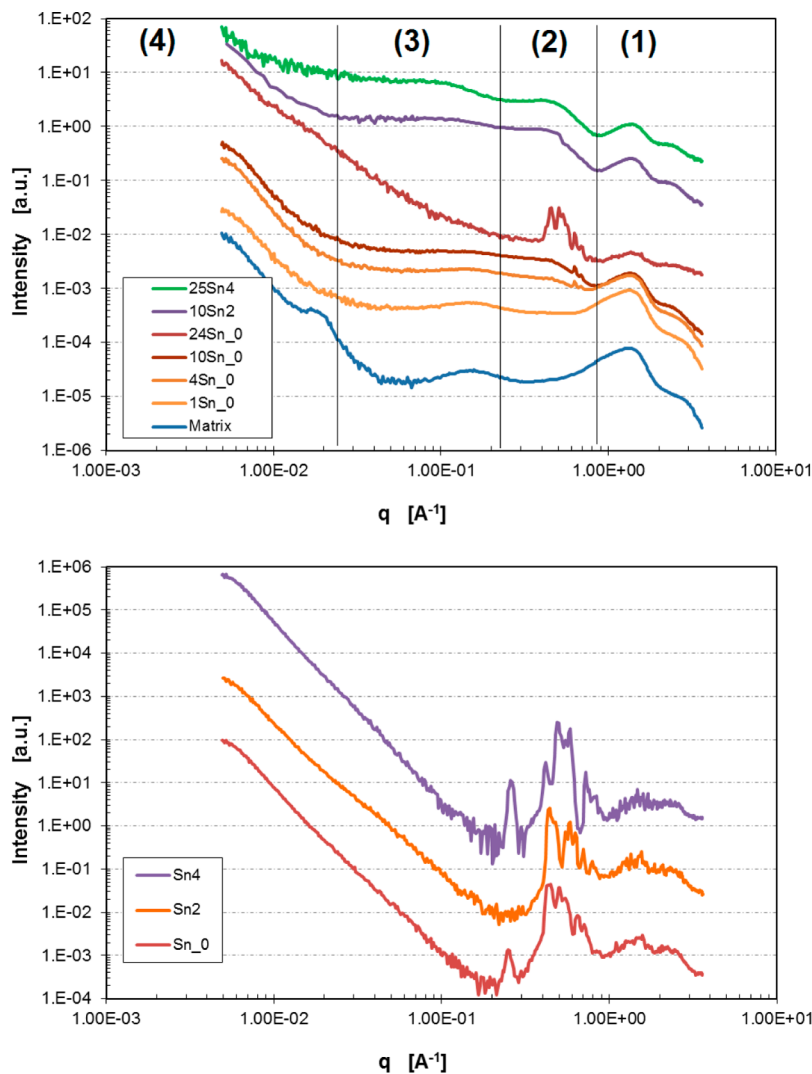


Figure 5. X-ray scattering patterns (SAXS + WAXS) of the neat matrix and of the hybrid resins with 1, 4, 10, and 24 wt % Sn₀, with 20 wt % (10 mol %) Sn₂, and 24 wt % (25 mol %) of Sn₄, which underwent the standard cure at 120 °C (top); for comparison, the scattering patterns of the neat cages Sn₀, Sn₂, and Sn₄ are also shown (bottom).

Table 4. Composition and the Results of the Extraction Tests of the Most Important Epoxystannoxane Resins

sample name	mol % of Sn cage	wt % of Sn cage	type of Sn cage	additional treatment	fraction of gel w_g^a	w_g^a of cages	w_g^a of matrix
matrix	0	0	none	NO	0.96	no	0.96
matrix-pcAr	0	0	none	180 °C/12 h, under Ar	0.85	no	0.85
matrix-ox	0	0	none	180 °C/12 h, in air	0	no	0
10-Sn ₀ -n	0	10	Sn ₀	NO	0.95	0.69	0.98
24-Sn ₀ -n	0	24	Sn ₀	NO	0.89	0.64	0.97
24-Sn ₀ -pcAr	0	24	Sn ₀	180 °C/12 h, under Ar	0.84	0.78	0.86
24-Sn ₀ -ox	0	24	Sn ₀	180 °C/12 h, in air	0.68	0.85	0.63
4-Sn ₂ -n	4	8	Sn	NO	0.97	0.97	0.97
10-Sn ₂ -n	10	19	Sn ₂	NO	0.95	0.95	0.95
10-Sn ₂ -pcAr	10	19	Sn ₂	180 °C/12 h, under Ar	0.92	0.98	0.91
10-Sn ₂ -ox	10	19	Sn ₂	180 °C/12 h, in air	0.87	0.98	0.86
25-Sn ₂ -n	25	40	Sn ₂	NO	0.81	0.83	0.80
25-Sn ₂ -pcAr	25	40	Sn ₂	180 °C/12 h, under Ar	0.85	0.88	0.83
25-Sn ₂ -ox	25	40	Sn ₂	180 °C/12 h, in air	0.78	0.82	0.75
10-Sn ₄ n	10	10	Sn ₄	NO	0.97	0.98	0.97
25-Sn ₄ -n	25	24	Sn ₄	NO	1.00	1	1
25-Sn ₄ -pcAr	25	24	Sn ₄	180 °C/12 h, under Ar	0.92	0.99	0.90
25-Sn ₄ -ox	25	24	Sn ₄	180 °C/12 h, in air	0.78	0.94	0.73

^aThe accuracy of the determination of the gel fraction was $\pm 1.5\%$.

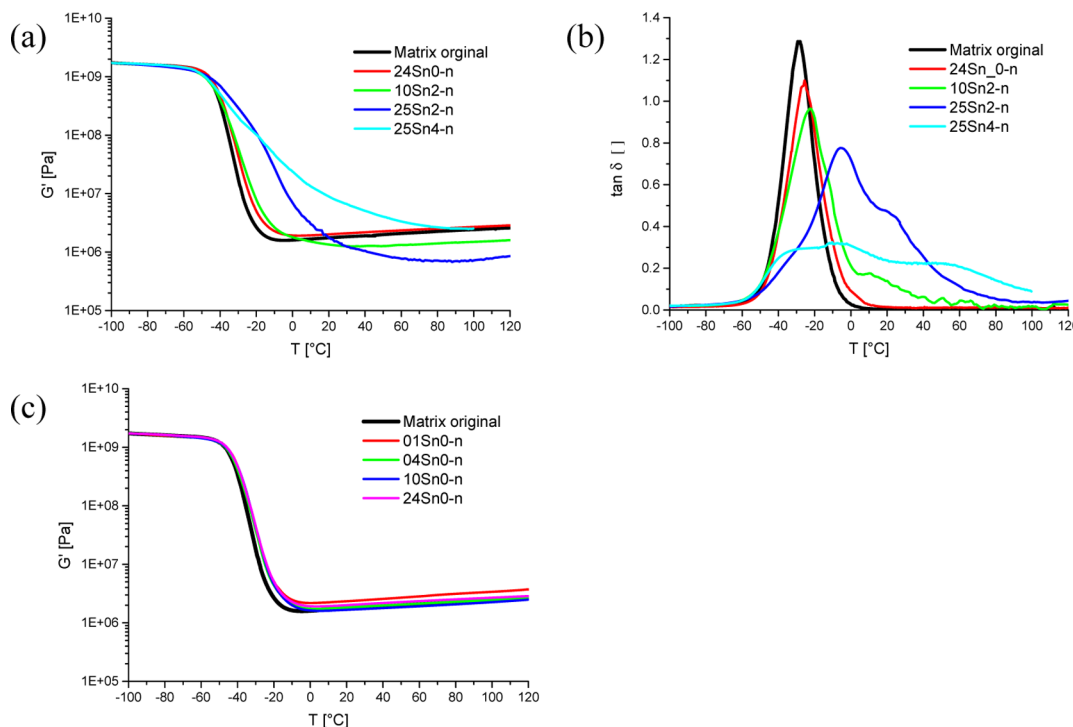


Figure 6. Normally cured ($120\text{ }^\circ\text{C}$) epoxystannoxane resins: Effect of stannoxyne cage functionality on the thermomechanical properties: shear storage modulus G' (a) and loss factor $\tan(\delta)$ (b) as a function of temperature; (c) effect of Sn_0 content, $G' = f(T)$.

scattering intensity increases linearly in the doubly logarithmic scale. This part of the scattering patterns can be correlated with the fractal dimensions of heterogeneities like single stannoxyne cages or their aggregates. The epoxystannoxane resins compared in Figure 5, top, all display a steep increase in the scattering intensity with decreasing scattering vector, consistent with a dispersion of spherical particles.

3.2.4. Extractability of the Dispersed Stannoxyne Cages. The efficiency of the incorporation of the Sn_0 , $\text{Sn}2$, and $\text{Sn}4$ cages into the epoxy matrix was investigated by extraction experiments. The overall gel fraction was determined via extraction with a 1:1 toluene–THF mixture, which effectively dissolves the components of the DGEBA–D2000 matrix as well as the neat stannoxyne cages. Additionally, ash analysis (stannoxyne conversion to SnO_2) was performed on selected samples, before and after extraction, in order to directly determine the change in cage content. The results were compared with extraction tests on the neat matrix.

The results of the extraction experiments, performed with selected DGEBA–D2000–stannoxyne resins containing Sn_0 , $\text{Sn}2$, and $\text{Sn}4$ cages, are shown in Table 4. It can be seen that the chemically bonded $\text{Sn}2$ and $\text{Sn}4$ cages are incorporated with a high efficiency and are difficult to extract. The incorporation of the linearly bonding $\text{Sn}2$ cage is especially efficient at medium and lower $\text{Sn}2$ concentrations, e.g., 4 mol % $\text{Sn}2$ (= 8 wt %), due to the high reactivity of $\text{Sn}2$ toward epoxies, combined with only a moderate decrease of the chemical cross-link density in the matrix (as linear $\text{Sn}2$ replaces branching D2000 in the copolymeric resin). The $\text{Sn}4$ cage is always highly efficiently incorporated, obviously due to its functionality as branching unit, in spite of its moderate reactivity. Interesting is the relatively low extractability of the nonbonding Sn_0 cage, the larger part of which stays in the matrix after the extraction. As a possible explanation it could be suggested that the large size of the Sn_0 cages in comparison to

the coiled elastic chains of the network mesh can result in a slow long-range mobility of the free cages. Additionally, also other effects might play a role like hydrogen bridging between the protons involved in the oxonium bonds in Sn_0 and the poly(propylene oxide) chains of the matrix, similar to the protonation reaction suggested in Scheme 9.

Annealing at $180\text{ }^\circ\text{C}$ under argon, which was performed in order to enforce stannoxyne cages’ oligomerization (see below), generally leads to a decrease of the gel fractions of the samples, obviously due to the thermal degradation of the matrix (as can be seen for the neat matrix, Table 4). As consequence of the cages’ oligomerization to larger domains, the partial gel fraction of the cages either stays practically unchanged ($\text{Sn}4$) or even increases in the case of Sn_0 and especially of $\text{Sn}2$, where additional chemical cross-links are formed by merger of $\text{Sn}2$ units.

The epoxystannoxane resins were also subjected to an oxidation treatment (see below: heating for 12 h at $180\text{ }^\circ\text{C}$ in circulating air), which was performed to assess the cages’ stabilizing effect. The gel fractions of all epoxystannoxane resins decreased after the oxidation treatment (see Table 4), but to a much smaller extent (24-Sn₀:0.89 → 0.68; 10-Sn₂:0.95 → 0.87; 25-Sn₂:0.81 → 0.78, 25-Sn₄:1.00 → 0.78) than in the case of the neat matrix, which becomes a soft soluble solid (w_g : 1 → 0). The gel fraction of the cages either did not decrease or decreased slightly in the resins with $\text{Sn}2$ (25-Sn₂:0.83 → 0.82; 10-Sn₂:0.95 → 0.98) and $\text{Sn}4$ (25-Sn₄:1.00 → 0.94), while it distinctly increased in epoxy- Sn_0 resins (24-Sn₀:0.64 → 0.85), in which the cages were newly attached to the matrix by covalent bonds, as result of oxidative cross-linking reactions. The partial gel fraction of the matrix decreased in all epoxystannoxane resins after the oxidation treatment.

3.2.5. Effect of the Stannoxyne Cages’ Dispersion on the Thermomechanical Properties. The effect of the dispersion of nonbonded (Sn_0), linearly bonded ($\text{Sn}2$), and branching

(Sn4) large-molecule-sized inorganic stannoxane cages on the thermomechanical properties of the copolymer- or blend-type hybrid resins based on the DGEBA-D2000 system is illustrated in Figure 6. Curves of the temperature dependence of the storage shear modulus (G' , see Figure 6a) are compared for epoxystannoxane resins after standard cure with approximately the same weight content of stannoxane: 24 wt % Sn₀ ("24Sn₀-n"), 20 wt % Sn2 (10 mol %, "10Sn2-n") and 24 wt % Sn4 (25 mol %, "25Sn4-n"). For comparison, the DMTA profile of the sample with 40 wt % (25 mol %, "25Sn2-n") is also depicted in Figure 6.

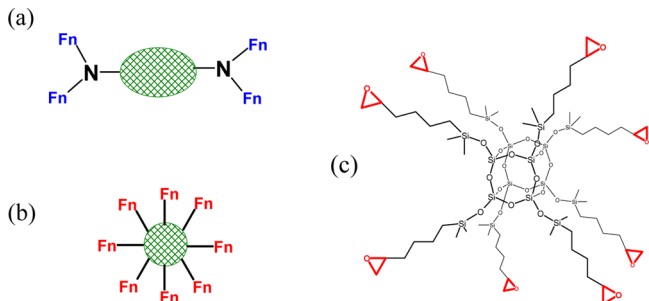
The analysis of the $\tan(\delta) = f(T)$ curves (see Supporting Information Figure 3 and comments) made possible the assignment of three thermal transitions in the studied epoxystannoxane resins: the free relaxation of the matrix (mainly D2000 chains) near -29 °C ($\tan(\delta)$ maximum), the relaxation of the topologically constrained matrix near -8 °C, and the relaxation of stannoxane-rich domains in the region 10–60 °C. The latter is not observed in the case of the nonbonded Sn₀ cage.

Sn4 Cage. From the comparison of the $G' = f(T)$ curves it can be concluded that the branching Sn4 cage displays the highest reinforcing effect at a given weight content: Markedly higher G' values can be observed for the sample 25-Sn4-n than for the neat matrix in the T range from -20 to +50 °C. An increase in the glass transition temperature T_g —defined as the temperature of the $\tan(\delta)$ maximum (see curves in Figure 6b)—by 24 ± 1 °C is also observed for 25-Sn4-n in comparison to the neat matrix.

It is of interest to compare the effect of the branching stannoxane cage Sn4 in epoxy copolymers with the effect of its lighter homologue POSS: The effect of the latter is discussed in several reviews.^{1,43–47}

Branching (typically octafunctional) POSS is a polyfunctional cross-linker, and hence it usually raises the modulus of the epoxy copolymers (which are often controversially called nanocomposites in the literature) in the rubber region, in extreme cases hard materials with no T_g are obtained.⁴⁸ On the other hand, the specific chemical structure of the matrix plays a decisive role: an increase in cross-link density (higher rubber region modulus) combined with a lower T_g (higher overall mobility) is often observed.^{49,26} In the case of the DGEBA-D2000-POSSe8 hybrid resin (organic–inorganic copolymer) with a branching POSS octaeoxide (POSSe8, see Scheme 10),

Scheme 10. Comparison of the Nanometer-Sized Branching Cages (a) "Sn4" ($F_n = (N\text{-})H$) and (b) of the Silicon-POSS Compound "POSSe8" ($F_n = \text{Epoxy}$); (c) Full Structure of POSSe8^a



^aThe uneven distribution of Sn4's functional groups on its surface is clearly visible.

studied by the authors previously,^{26,27} the same matrix was used like in this work. The observed decrease in T_g can be explained by the replacement of the rigid DGEBA-N-DGEBA-N- chains of the matrix (see Scheme 6) by single POSS units or by bonded-together small groups of POSS (a detailed discussion of the structure is given in ref 27). These rigid spherical units (acting as simple polyfunctional cross-linking points) are connected by the elastic D2000 chains.

The interpenetrating DGEBA-N-DGEBA-N- structure, which immobilized the neat matrix, is partly or is completely (at 100 mol % POSSe8) replaced by spherical polyfunctional cross-links. The missing immobilization results in the observed T_g decrease. Additionally, the high cross-linking functionality of POSSe8 is also moderated by the possibility of a specific reaction of POSSe8 with the amino component of the matrix, D2000: Two epoxy "arms" of POSSe8 can react with the same NH₂ group of D2000, thus reducing the effective functionality of both components (see ref 27). As consequence, a smaller than theoretically expected increase in rubber modulus is observed after POSSe8 incorporation into the DGEBA-D2000 matrix (see Figure 7).

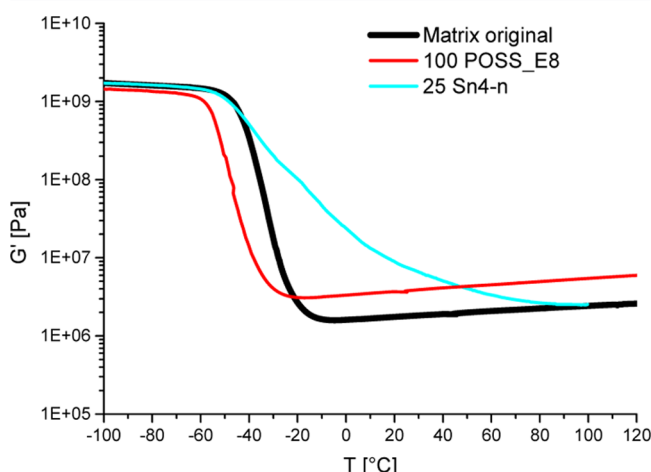
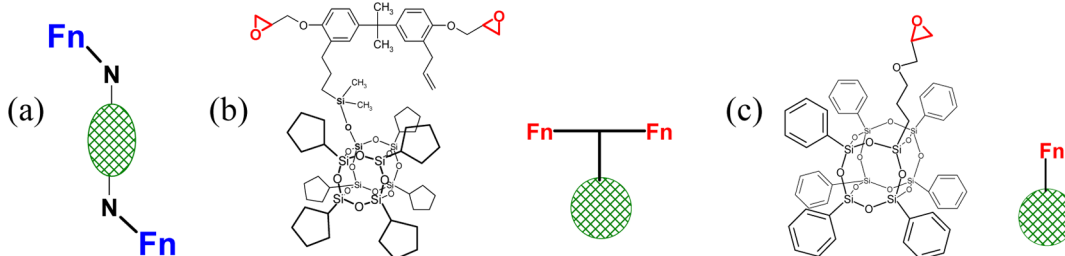


Figure 7. Effect of branching inorganic cage comonomers "Sn4" (25 mol % ≡ 40 wt %) and "POSSe8" (100 mol % ≡ 31 wt %) on the thermomechanical properties of the DGEBA-D2000 matrix, $G' = f(T)$.

Prior to the authors' discussed previous work, Laine et al. studied a similar epoxy-POSSe8 system with a much narrower network mesh,^{50,43,51} based on DGEBA, diaminodiphenylmethane (DDM), and a POSSe8 epoxide very similar to the one shown in Scheme 10c, but with propyloxyglycidyl functional arms in place of epoxy hexyl ones. Also in the case of this more densely cross-linked epoxy network, the POSS octaeoxide comonomer caused an increase in the rubber modulus (a marked one) as well as a decrease of the glass transition temperature. In the case of the stoichiometric POSSe8-DDM composition, the glass transition was already very faint. In extreme cases of very highly cross-linked matrices, the relatively large polyfunctional POSS can cause a decrease of cross-link density (lower rubber modulus) and simultaneously (via segmental mobility of its functional arms) a lowering of T_g .⁵² The above examples illustrate the high importance of the chemical structure details for the final effect of branching large-molecule-sized inorganic cages, like POSSe8 or Sn4.

If the shape, functionality (two NH₂ groups), and the molecular weight of Sn4 are considered, it can be found very

Scheme 11. Inorganic Cages, Which Are Incorporated into the Polymer Backbone (“Sn2” (a), Fn = (N–)H), as a Dangling Unit near the Backbone (“CpPOSSdgeba”, (b), Fn = Epoxy), or as a Dangling Unit Which Simultaneously Disrupts the Backbone (“PhPOSSe1”, (c), Fn = Epoxy)



similar to a coiled D2000 molecule frozen in this conformation. As Sn4 partly replaces D2000 in the DGEBA-D2000-Sn4 resin, little effect on mechanical properties could be expected at a first approach, especially no change in the rubber modulus, because Sn4 and D2000 possess the same amino-H functionality (four) and occupy approximately the same volume. In view of Sn4's rigidity, elastic inactivity, and higher density than D2000, an increase in T_g and a slight increase in rubber modulus could be expected at high Sn4 concentrations. In the absence of Sn4–Sn4 or Sn4–matrix interactions, if only the cross-linking functionality were important, the glass transitions of DGEBA-D2000-Sn4 resins could be expected to be sharp, similarly like in POSSe8 epoxy copolymers. The observed glass transition of the 25-Sn4-n resin ($G' = f(T)$ curve) is “gradual”; it occurs between -30 and $+70$ °C. This is in contrast with the “stepwise” glass transitions of the neat matrix (between -30 and $+10$ °C) or of the DGEBA-D2000-POSSe8 resin (between -50 and -10 °C). In accordance with expectation, the equilibrium modulus in the rubber region of the 25-Sn4-n resin (at $T > 80$ °C) is practically the same like in the case of the neat matrix. In the T region between -30 and $+70$ °C, a specific reinforcing effect can be attributed to Sn4, originating mainly in Sn4–matrix interactions (primary and secondary Sn4 aggregates intercalated by matrix, see Scheme 15, left) which was first reported and discussed in detail in ref 41. The mentioned interactions are disrupted at $T > 80$ °C (relaxation of the secondary aggregates). In contrast to POSSe8 with functions evenly distributed on its surface (Scheme 10c), the Sn4 cage has a lower functionality, and its functions (amino protons) are distributed highly unevenly, in pairs on the axial substituents (Scheme 10a). This makes matrix–Sn4 interactions possible, although Sn4 is a cross-linker.

Sn2 Cage. At a similar stannoxane weight content like in 25-Sn4-n, the linearly bonded Sn2 cage (in 10-Sn2-n) exhibits a much weaker reinforcement, comparable to the one caused by the nonbonded Sn₀: T_g increases only slightly, by 7 ± 1 °C ($\tan(\delta)$ curves in Figure 6b; the shift of the $G' = f(T)$ curve to higher temperatures is also clearly visible in Figure 6a), but the modulus in the rubber region moderately decreases. At 40 wt % (25-Sn2-n), both effects of Sn2 are much stronger, the T_g increases by 20 °C, and the modulus in the rubbery region decreases significantly as well. The $G' = f(T)$ curves of the epoxy-Sn2 resins display a much steeper step near T_g (similarly like the neat matrix) than is observed for their Sn4 analogues. This simple behavior indicates that the main effects of Sn2 are a moderate immobilization of the matrix and a reduction of the cross-link density.

Several reviews^{1,43–45} discuss the effect of POSS analogues of the studied stannoxane cages, incorporated as dangling units

(see Scheme 11). This bonding of POSS is similar to, but not identical with, the bonding of Sn2 (see comparison in Scheme 11), which is incorporated directly in the backbone of the DGEBA-N-DGEBA-N-chains of the matrix (see Scheme 6). If the inorganic cage is incorporated as dangling unit or as a part of the backbone, eventual cage–cage and cage–elastic chain interactions are easily possible. Suitable dangling POSS units were found to raise $T_g^{53,54}$ and the rubber modulus²⁶ as well.

A highly efficient mechanism for this reinforcement is the formation of physical cross-links via POSS–POSS interactions,^{55,26} although other effects are also known to play an important role, like the inertia of the heavy POSS⁵⁵ and topological constraint^{56,27,28} by single POSS units or nano-aggregates. The substituents attached to the surface of dangling POSS units are of key importance for the possibility of physical cross-linking via POSS–POSS interactions: Strongly crystallizing substituents like phenyl and cyclohexyl cause a strong reinforcement, while “soft” substituents like isoctyl lead to epoxy-POSS resins which are plastified.^{54,26} Also, the exact bonding of dangling POSS, i.e., an eventual reduced functionality (Scheme 11c), can reduce the reinforcing effect (Figure 8: weaker reinforcement by PhPOSSe1 than by CpPOSSdgeba).

In the case of Sn2 and its *n*-butyl substituents, crystallization is not enforced like with phenyl or cyclohexyl, and hence no increase in rubber modulus is observed, while on the other hand, the reduction of cross-link density caused by the replacement of amino-H-tetrafunctional D2000 with the

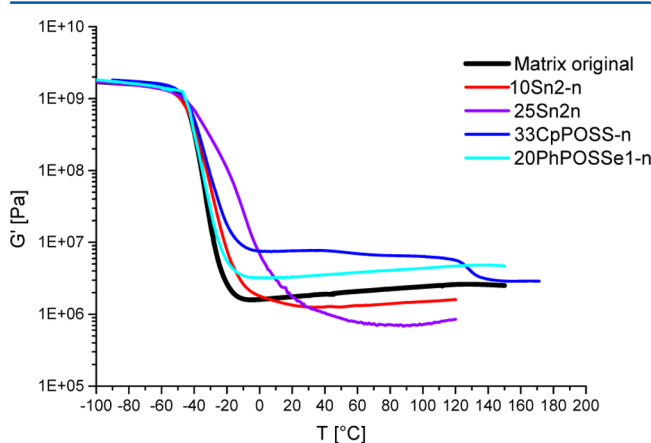
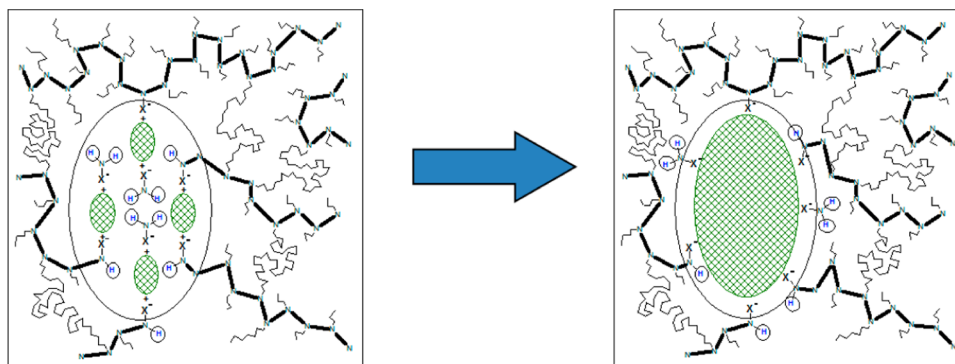


Figure 8. Effect of linearly bonded Sn2 cage comonomer (10 and 25 mol % \equiv 19 and 40 wt %) on the thermomechanical properties of the DGEBA-D2000 matrix, compared with the effect of roughly similarly incorporated silicon–POSS compounds: 33 mol % (\equiv 27 wt %) CpPOSSdgeba and 20 mol % (\equiv 25%) PhPOSSe1.

Scheme 12. Stannoxane Polymerization at Elevated Temperatures on the Example of a Small Multiplet Domain

amino-H-bifunctional Sn2 causes a decrease of rubber modulus. On the other hand, the incorporation of the heavy Sn2 into the rigid DGEBA-N-DGEBA-N- chains which play an immobilizing role in the matrix, and possibly also the interactions of Sn2 and the elastic D2000 chains, cause a distinct increase in T_g , which can be considered as a specific reinforcing effect of Sn2. If only the chemical functionality of Sn2 played a role, then it would be expected to act as a chain extender of the epoxy component DGEBA, thus lowering G' and T_g (more conformational mobility in the rigid DGEBA-N- DGEBA-N- chains).

Figure 8 compares the reinforcing effects of Sn2 in 10-Sn2-n and 25-Sn2-n with the effect of CpPOSSdgeba (diepoxyde) and Ph7POSSe1 (monoepoxide) in the same matrix: Sn2 causes an increase in T_g combined with a decrease in the rubber modulus, while both POSS derivatives display a reinforcement by physical cross-linking, which is more efficient in the case of CpPOSSdgeba because the monofunctional Ph7POSSe1 reduces the cross-link density of the matrix. On the other hand, CpPOSSdgeba displays a lower melting point of the physical cross-links. A slight increase in T_g is also observed for both POSS cages, similar to the one observed in 10-Sn2-n which contains a similar weight fraction of inorganic cages.

***Sn₀* Cage.** The nonbonding cage Sn₀ causes only a slight reinforcement of the matrix (see Figure 6c): At 24 wt % Sn2, an increase in T_g by only 5 ± 1 °C is observed as well as a slight increase in the modulus in the rubber region. The hybrid resins (blends) with 1, 4, and 10 wt % display very similar DMTA profiles like 24-Sn₀-n (Figure 6c). Interestingly, the reinforcing (antiplasticizing) effect of Sn₀ is the strongest at 1 wt %, in the only epoxy-Sn₀ resin which displayed a homogeneous morphology. At higher Sn₀ contents, the stannoxane effect on T_g and G' diminishes, although between 10 and 24 wt % G' increases slightly again, probably due to hydrodynamic toughening by Sn₀ crystallites which occupy a considerable volume fraction at 24 wt % Sn₀.

The effect of nonbonded POSS analogues of Sn₀ in polymers is discussed in several reviews.^{1,43–45} For example, in high-density polyethylene, the highly crystallizing octamethyl-POSS (POSSme8) was found to disperse monomolecularly at very low contents (below 0.5 wt %), while at contents around 5 wt % the POSS units start to agglomerate and cause a physical gelation of the polymer melt.⁵⁷ A similar behavior was observed also with POSSme8 in polyethylene–polypropylene copolymer, in which finely dispersed POSSme8 units at low weight contents can cause physical gelation of the polymer melt.⁵⁸ This behavior was assigned to interactions between POSS units and nanocrystallites in the material, rather than to POSS–polymer interactions.⁵⁸ In case of nonbonding POSS which

does not tend to crystallization, e.g., octaisooctyl-POSS (weak POSS–POSS interactions), the reinforcement at low concentrations is not observed.⁵⁹ The behavior of Sn₀ in the DGEBA-D2000 matrix is most likely very similar to the effect of its POSSme8 analogue in the above-discussed cases (crystallization observed by TEM). The small but distinct reinforcing effect of Sn₀ is the strongest at a concentration which is so low that Sn₀ just stops to form crystallites visible by TEM. Interactions of Sn₀ units and small nanocrystallites as discussed above for POSS are most likely occur at this Sn₀ concentration (compare Figure 4). The associated Sn₀ units and nanocrystallites then would act as physical cross-links and as immobilizing structures on matrix segments, thus causing the observed slight increases in T_g and rubber modulus. At higher Sn₀ contents, the amount of freely dispersed Sn₀ might be smaller than in 1-Sn₀-n due to Sn₀ accretion by nano-domains and crystallites.

3.3. Cages' Oligomerization and Its Effects in the Hybrid Resins. 3.3.1. Chemistry of the Stannoxane Rearrangement to Larger Structures.

The tendency of the butylstannoxane dodecamer cages to rearrange to oligomers or polymers at elevated temperatures (Scheme 12) was already reported in earlier work.^{37,41}

One of the aims of this work was to compare the freely dispersed, linearly bonded, and branching stannoxane cages Sn₀, Sn2, and Sn4 in this respect. The neat cages melt at 198 °C (Sn₀), 113 °C (Sn2), and 253 °C (Sn4). At 255 °C, all the cages melt and subsequently polymerize in less than 5 min, Sn₀ somewhat slower than Sn4, while Sn2 melts and polymerizes instantly at this temperature (experiment: NMR capillary with 30 mg of sample, immersed in a constant-T oil bath). According to the authors' previous results,⁴¹ a nearly complete stannoxane oligomerization can be achieved by a prolonged (12 h) annealing under argon at 180 °C, while the thermal damage to the epoxy matrix is relatively small after such a treatment. In order to avoid oxidative stannoxane–matrix cross-linking, which represents a different and important chemical reaction (see below), the cages' oligomerization in the studied epoxystannoxane resins was always carried out via heating under argon at 180 °C for 12 h (“annealing under argon”).

In the case of soluble stannoxane cage derivatives, their gradual polymerization can be followed by means of ¹¹⁹Sn NMR spectroscopy as the decrease of integrals of the two ¹¹⁹Sn peaks which characterize the cage structure, at –273 ppm (5-coordinated equatorial Sn atoms on the ellipsoid cage) and at –453 ppm (6-coordinated Sn atoms on “polar circles” of the cage), as reported previously by the authors.⁴¹ The stannoxane

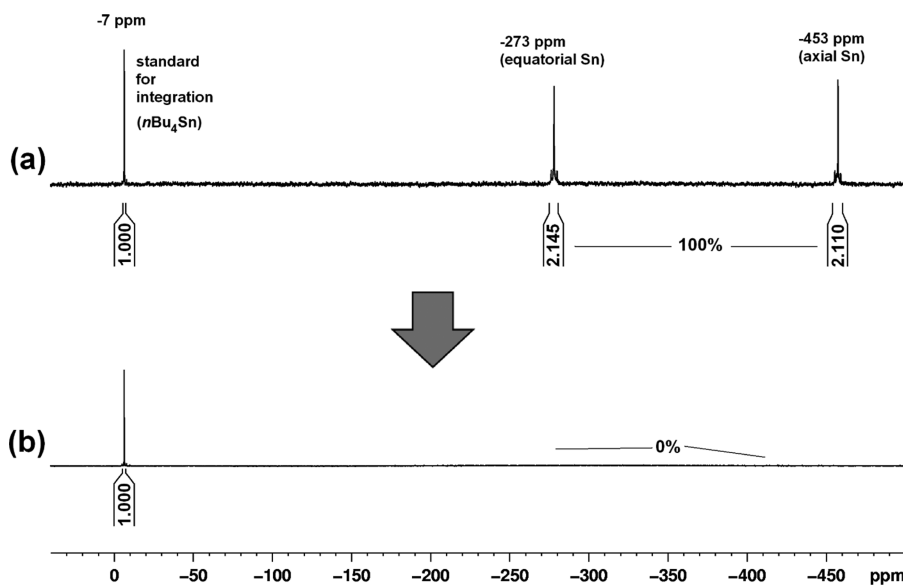
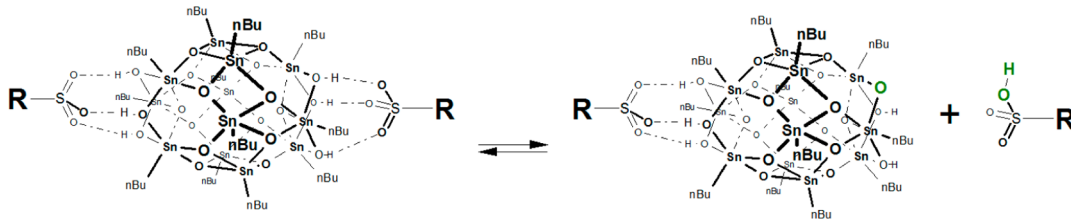


Figure 9. Rearrangement of stannoxane clusters to larger structures observed by means of ^{119}Sn NMR on the example of Sn4: after 30 min annealing at $240\text{ }^\circ\text{C}$ under argon, the characteristic peaks of the stannoxane cage disappear.

Scheme 13. Proposed Starting Step of the Stannoxane Cages Oligomerization: Oxonium Salt Dissociation



structures formed by the polymerization display long NMR relaxation times, in addition to irregularity-induced signal broadening; hence, their signals are not detectable under the standard measurement conditions.³⁷ As example, the ^{119}Sn NMR spectra of neat Sn4 before and after polymerization at $255\text{ }^\circ\text{C}$ are shown in Figure 9, with tetrabutylstannane as integration standard.

The mechanism of the stannoxane cage polymerization recently suggested by the authors⁴¹ begins with the dissociation of the oxonium ionic bonds, by which the axial substituents are attached to the cage (Scheme 13), in analogy to ammonium salts (e.g., NH_4Cl) dissociation upon the latter's sublimation. Subsequently, the destabilized cage is expected to undergo rearrangements, reprotonations by the sulfonic acid (former axial substituent) under formation of new oxonium bonds at different than original positions. Finally, the defect and reactive cages would collide and merge to larger structures. The importance of acidic protons for reorganization of stannoxane structures can also be seen in the example of the cage synthesis from the polymeric $[\text{R}-\text{Sn}(\text{O})\text{OH}]_n$ (see above, Scheme 4: an excess of the sulfonic acid reactant is used as catalyst in that reaction³⁷).

The stability of the oxonium bonds in Sn₀, Sn2 and Sn4 was investigated by means of ^1H NMR spectroscopy (see Supporting Information Figures 4 and 5 and attached comments). Sn₀ and Sn4 display a sharp resonance peak of the hydroxyl groups of the cages which take part in the oxonium bonds (Supporting Information Figure 4). In contrast to this, Sn2 displays a very broad and flat peak of a joint signal of the cage OH groups, of SO_3H groups, and of the axial

substituents' amino protons. A fluctuation of the functional substituents to the Sn2 cage is hence suggested as shown in Scheme 14.

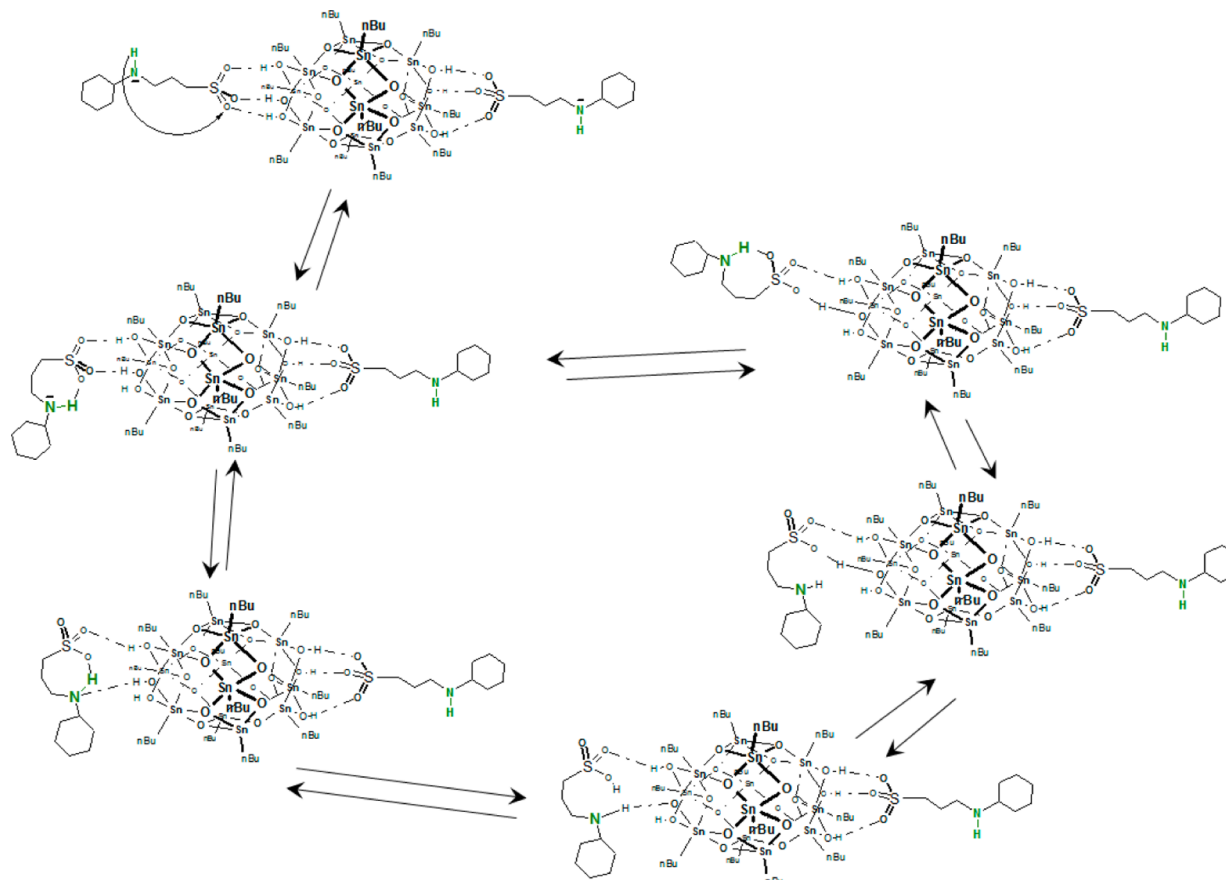
The observed fluctuations of the axial sulfonate substituents of Sn2 (Scheme 14) would explain the comparably low melting point of Sn2 in contrast to Sn₀ and Sn4, in spite of the strongly crystallization-supporting cyclohexyl groups in the structure of Sn2. The unusually high reactivity of Sn2 toward epoxy groups (also the catalysis of epoxy-ROP) as well as the short-range mobility of Sn2 at elevated temperatures, which will be discussed below, also can be explained by the fluctuating oxonium bonds.

Temperature-dependent FT-IR experiments (see Supporting Information Figures 6 and 7 and attached comments) confirmed the different stability of the oxonium bonds: $\text{Sn}_0 > \text{Sn4} \gg \text{Sn2}$. The experiments were carried out on neat stannoxane samples, and the temperature-dependent changes of the OH, NH, and SO_3 vibration peaks were evaluated. Sn₀ and Sn4 were practically unchanged upon heating to $120\text{ }^\circ\text{C}$, while the spectra of Sn2 displayed changes already at $60\text{ }^\circ\text{C}$.

3.3.2. Morphology Changes after Stannoxane Oligomerization. The morphology changes in the DGEBA-D2000-based resins containing Sn₀, Sn2, and Sn4 after the cages' polymerization (via annealing under argon at $180\text{ }^\circ\text{C}$) were studied by means of transmission electron microscopy.

The epoxy-Sn₀ resins (blends) display practically no changes in morphology after the cages' polymerization, the fine dispersion at 1 wt %, or the crystallites at higher contents remained unchanged (see Supporting Information Figure 8).

Scheme 14. Proposed Proton Exchange Reactions of the Sn₂ Cage in CDCl₃ Solution, in Which a Proton Is Exchanged between OH, NH, and SO₃H Groups^a



^aThe oxonium bonds are more stable and do not fluctuate in Sn₂ and Sn4.

The epoxy-Sn₄ resins (copolymers) with DGEBA-D2000 do not change their morphology after the annealing under argon (TEM).⁴¹ This is obviously due to the specific phase structure of the epoxy-Sn₄ resins, before and after cages' oligomerization, which was investigated in detail in previous work⁴¹ and which is illustrated in Scheme 15.

Epoxy-Sn₂ resins (copolymers) surprisingly display a distinct change of morphology after the annealing at 180 °C (Figure 10). In place of the expected merger of occasional neighboring Sn₂ units to larger, but still very small structures, a strong

Scheme 15. Previously Reported⁴¹ Polymerization of Primary Domains of Sn₄ Inside of Secondary Aggregates, Which Has Practically No Effect on Morphology or on Mechanical Properties

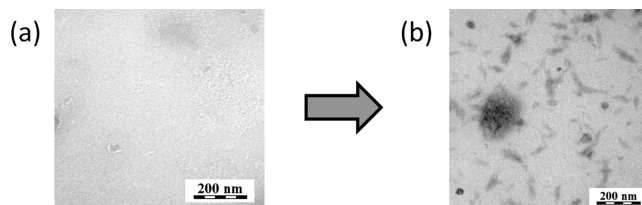
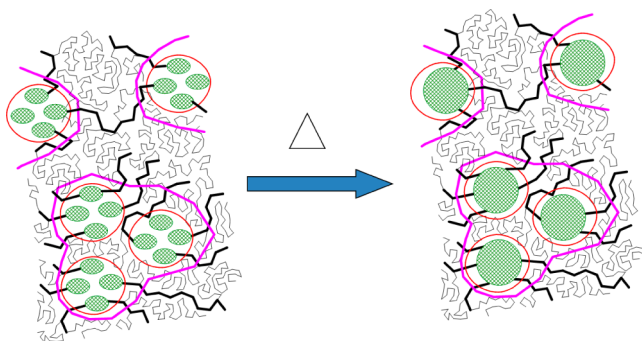
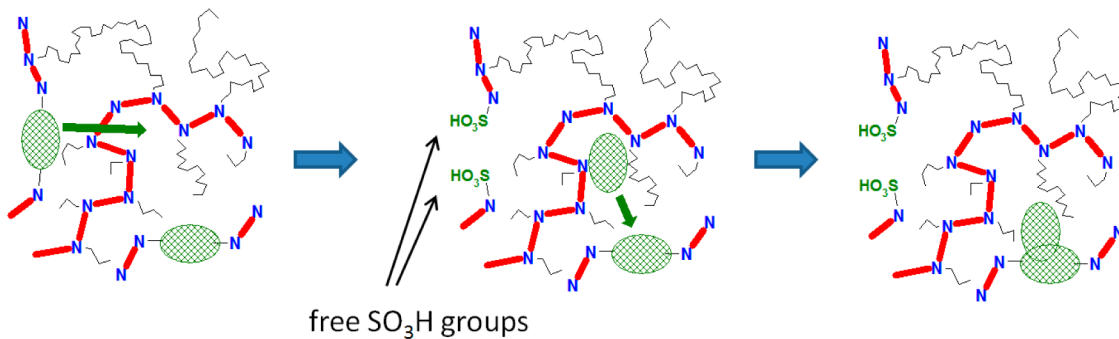


Figure 10. TEM images of the 10-Sn₂ hybrid resin before and after annealing under argon: (a) 10-Sn₂-n (after standard cure); (b) 10-Sn₂-pcAr (after annealing).

nanophase separation is observed: Sn₂-rich domains containing up to several hundred Sn₂ cages are formed, as can be seen on the example of the resin with 20 wt % Sn₂ (10 mol %, see Figure 10). This nanophase separation can be seen at all Sn₂ concentrations and has especially marked effects at weight loads of 20 wt % and more.

The morphology change resembles a phase separation in an originally vitrified matrix, which upon heating would lead to phase separation of mutually dissimilar copolymer blocks. However, the matrix is not vitrified at room temperature or at the temperature of the standard sample cure (synthesis: 3 days at 120 °C) which precede the annealing experiments: its T_g is -22 °C (10-Sn₂-n). Hence, an eventual Sn₂ phase separation prior to annealing is not hindered by a vitrified matrix. Furthermore, the phase separation of Sn₂ observed after annealing leads to Sn₂-rich domains (15 × 80 nm, see Figure

Scheme 16. Suggested Mechanism of the Nanophase Separation of the Finely Dispersed Sn₂ Cages during the Postcure under Argon: Easy Dissociation of Oxonium Bonds Makes Possible the Cages' Movement, Collisions, and Merger to Larger Domains



10) and to interdomain distances (100–200 nm), which are orders of magnitude larger than the Sn₂ cages (ca. $2.3 \times 2.3 \times 4.7$ nm with substituent shell). The latter also were not incorporated as Sn₂ sequences but as single units, and their segmental mobility is highly restricted by their incorporation in the rather rigid DGEBA-N-DGEBA-N-chains (see Scheme 6). Sn₂ is also practically inextractable from the epoxy-Sn₂ resins at room temperature (see Table 4). The Sn₂ separation upon annealing hence can be only reasonably explained by Sn₂ dissociation from its bonding sites at 180 °C and by its subsequent 100 nm range mobility, as suggested in Scheme 16. Such a mobility is not observed for Sn₄. The investigations of the oxonium bonds to the functional substituents (FT-IR, ¹H NMR) which are discussed above indeed indicate that the oxonium bonds in Sn₂ are markedly more labile than in Sn₄ or Sn₀. Because of the low solubility of Sn₀ in the matrix, this nonbonded and hence mobile cage is either very thinly dispersed or aggregated to large crystallites, so that its eventual mobility in the matrix does not produce visible (TEM) morphology changes.

3.3.3. Thermomechanical Properties after Stannoxane Oligomerization (DMTA). The effect of stannoxane cage polymerization on the thermomechanical properties of DGEBA-D2000-based resins containing Sn₀, Sn₂, and Sn₄ is illustrated in Figures 11 and 12.

Generally, it can be observed, that the polymerization of the Sn₄ cages in their domains (see Scheme 15) practically does

not change the thermomechanical properties of the DGEBA-D2000-Sn₄ resins (Figure 12c), as was discussed in detail in a previous work.⁴¹ The slight change in the DMTA profile of the sample with 24 wt % Sn₄ after the annealing under argon is connected with the thermal degradation of the epoxy matrix. As can be concluded from Figure 11, Sn₄ is the strongest-reinforcing stannoxane among the investigated ones at a given weight amount, also after the cages' polymerization.

The polymerization of the Sn₂ cages leads to a small change in the DMTA profiles at weight loads of 20 wt % and lower (see sample 10-Sn₂-pcAr in Figure 11, in comparison to 10-Sn₂-n in Figure 6). At high Sn₂ loadings (25-Sn₂-pcAr), the annealed hybrid resin displays a broadened glass transition (gradual G' decrease with T), probably due to the interaction of the larger stannoxane domains with the matrix and to stannoxane domains' thermal relaxation. The equilibrium rubber modulus did not increase after the annealing (25-Sn₂-pcAr), obviously due to the above-discussed nanophase separation of Sn₂, which must be inevitably connected with the loss of some of the functional substituents. Additionally, the above-discussed fluctuating oxonium bonds from Sn₂ domains to the functional substituents could possibly be able to dissociate under stress, especially at higher temperatures.

The polymerization of the nonfunctional Sn₀ cages in their domains or their thermal rearrangement in the molecularly dispersed form has only a very small effect on the thermomechanical properties of the DGEBA-D2000-Sn₀ resins. Nevertheless, some trends can be observed: the weak reinforcement (G') by Sn₀ in the rubber region disappears (Figure 12d): Practically identical $G' = f(T)$ curves are obtained for neat matrix and the epoxy-Sn₀ resins after annealing. The irregularity of the thermally rearranged Sn₀ cages probably minimizes their tendency to crystallize or to form branched associates. The originally narrow peaks of the curves $\tan(\delta) = f(T)$ become broader (Figure 13b), more so than in the case of the annealed neat matrix, especially at higher Sn₀ contents (compare with Figure 6, bottom). This broadened transition might be connected with the unsharp borders of Sn₀ domains after annealing, which can be observed by TEM (Supporting Information Figure 8) and which are possibly caused by irregular stannoxane structures interpenetrating the matrix near Sn₀ domain borders.

3.4. Oxidation Resistance of the Epoxystannoxane Resins. In their recent work,⁴¹ the authors found that the butylstannoxane dodecamer cages undergo oxidative cross-linking reactions (see Scheme 17) in epoxy matrices containing poly(propylene oxide) chains and that these reactions counteract the oxidative degradation of the matrices.

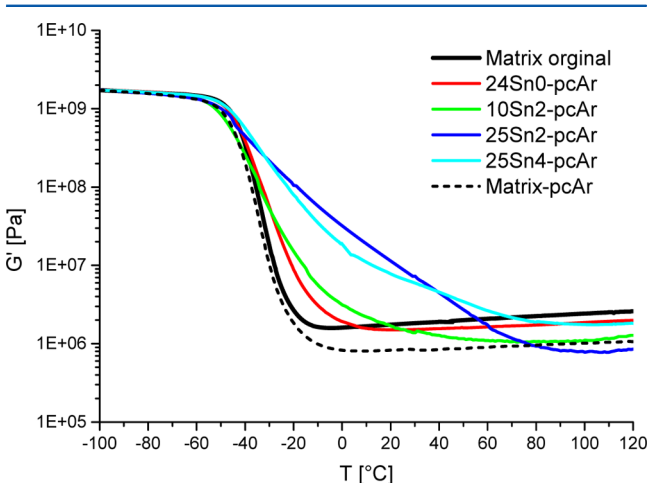


Figure 11. Epoxystannoxane resins after annealing under argon (cages' polymerization): effect of cages' functionality on the thermomechanical properties: Shear storage modulus G' as a function of temperature.

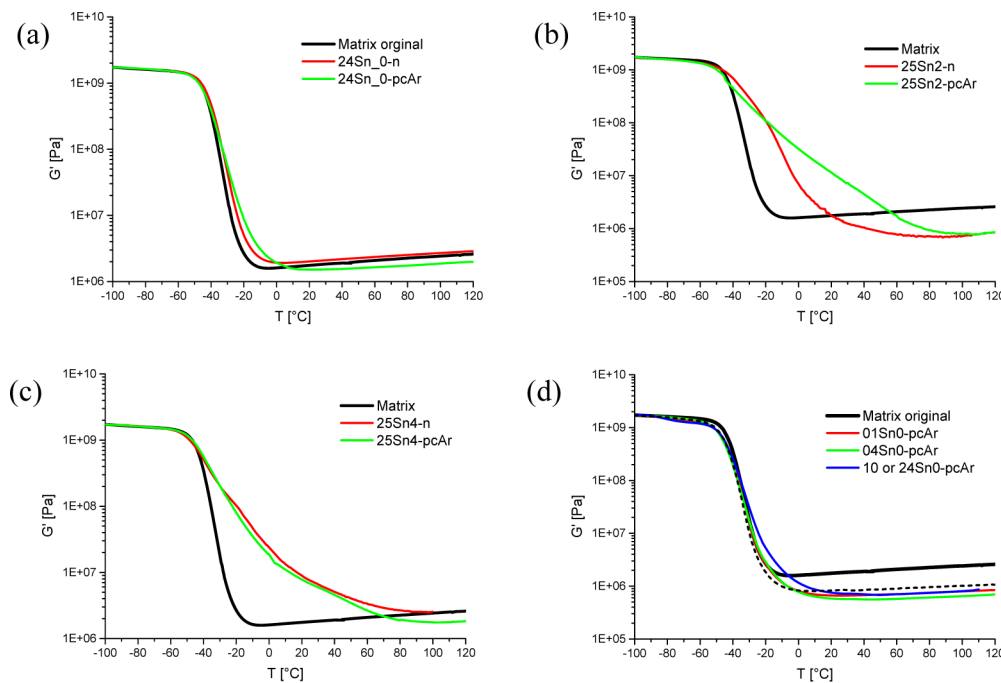


Figure 12. Effect of stannoxane cages polymerization on the thermomechanical properties after annealing under argon, on the example of the epoxystannoxane resins 24-Sn₀ (a), 25-Sn₂ (b), and 25-Sn₄ (c): Shear storage modulus G' as a function of temperature; $G' = f(T)$ for different Sn₀ contents after annealing under argon (d).

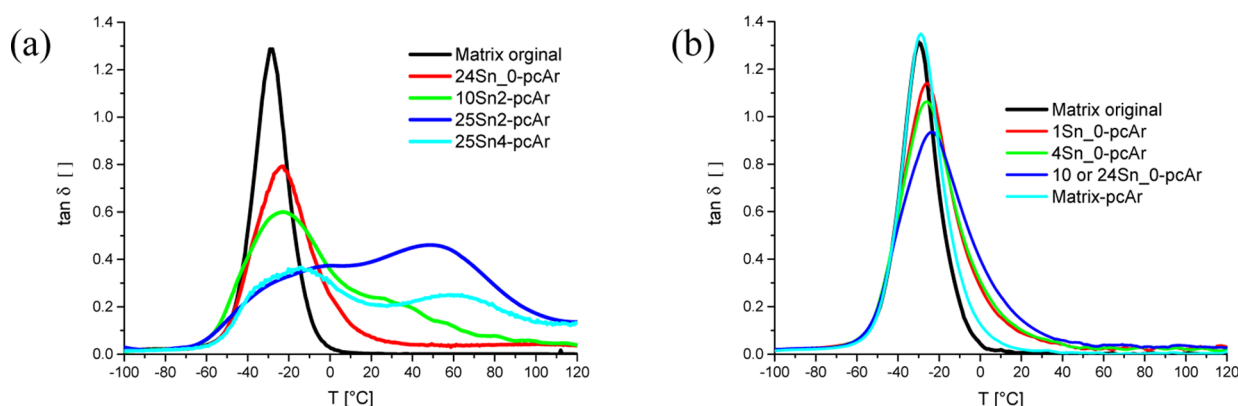


Figure 13. Loss factor $\tan(\delta)$ as a function of temperature (thermal transitions) after annealing under argon (cages' polymerization): (a) effect of stannoxane functionality; (b) effect of different Sn₀ contents.

The effect of this chemical activity of the cages especially strongly influenced the thermomechanical properties of the epoxystannoxane resins. The reactions were shown⁴¹ to involve cross-linking between cages and matrix and cage–cage cross-linking. In order to compare the antioxidant effect of Sn₀, Sn₂, and Sn₄ in hybrid resins based on DGEBA-D2000, the tested samples were subjected to an oxidation treatment consisting of heating in circulating air at 180 $^{\circ}$ C for 12 h. This procedure was established as “standard oxidation treatment” because after its completion, the gel fraction of the neat DGEBA-D2000 matrix decreases to zero and the matrix nearly becomes liquid.

3.4.1. Morphology Changes after Oxidation Treatment. The morphology of the hybrid resins containing Sn₀ and Sn₄ after the oxidation treatment (not shown) does not display any changes visible by TEM: The samples remain highly homogeneous, like before the oxidation.

In the oxidized epoxy-Sn₂ resins (copolymers), a phase separation can be observed (Figure 14), although to a much smaller extent than in the case of the epoxy-Sn₂ resins annealed under argon. Small spherical domains sized 5–15 nm appear in the oxidized resin 10-Sn₂-ox. The thermally induced nanophase separation and the short-range movement of the Sn₂ building blocks (which were both observed under the conditions of anaerobic annealing) are obviously suppressed by the oxidative cross-linking reactions, which lead to a strong covalent attachment of the Sn₂ cages to the matrix, and thus prevent their further movement.

3.4.2. Thermomechanical Properties after Oxidation Treatment. The epoxystannoxane resins which contain higher loadings of finely dispersed cages display a very strong additional reinforcement after the oxidation treatment. At higher stannoxane contents (around 20 wt %), the Sn₄ cage is again the strongest reinforcing agent, followed by Sn₂ and Sn₀ (see Figure 15). The nonbonding Sn₀ cage becomes

Scheme 17. Oxidative Cross-Linking Reactions of the Stannoxane Cages with the Matrix and with Each Other, As Proven by ^1H NMR Experiments in Previous Work⁴¹

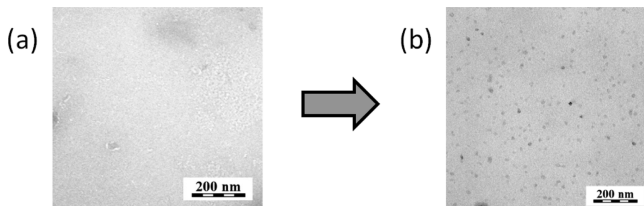
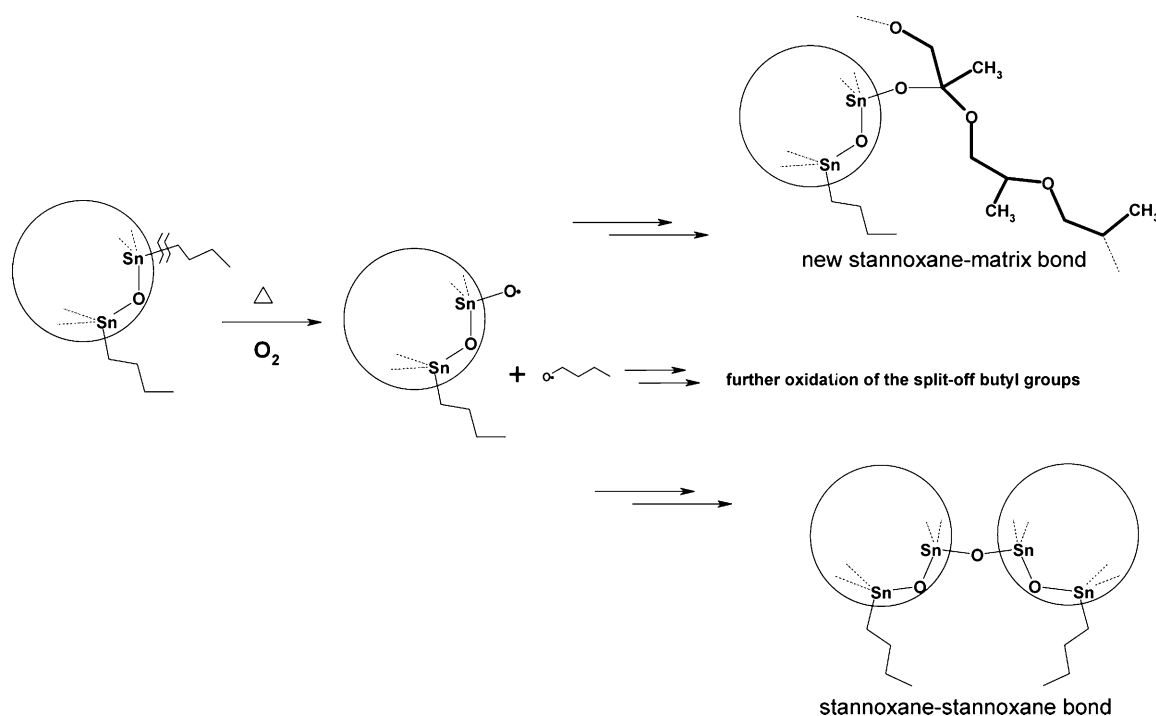


Figure 14. Effect of the oxidation treatment on the morphology of the 10-Sn2-n composite which transforms into the sample 10-Sn2-ox as observed by TEM: (a) the normally cured sample; (b) the oxidized one.

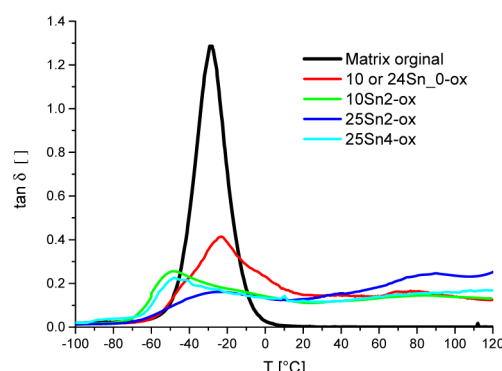
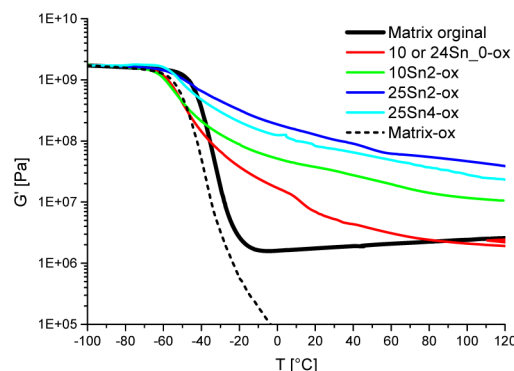


Figure 15. Epoxystannoxane resins containing Sn₀, Sn2, and Sn4 cages after oxidation treatment: effect of cage functionality on the thermomechanical properties: Shear storage modulus G' (top) and loss factor $\tan \delta$ (bottom) as a function of temperature.

covalently attached to the matrix, as result of the oxidative cross-linking reactions (characteristic shape of the $G' = f(T)$ curve). Because of poor Sn₀ dispersion at higher loadings (e.g., 24 wt %), this stannoxane cage causes a much smaller reinforcement after the oxidation treatment than Sn2 or Sn4 at similar contents. In contrast to the normally cured epoxy-Sn₀ resins, the oxidized ones display a similar phase transition behavior (see $\tan(\delta) = f(T)$ curves, Figure 15) like the hybrid resins with chemically bonded stannoxane cages Sn2 and Sn4: A broad transition region of a stannoxane-rich phase is observed in the oxidized epoxy-Sn₀ resins.

At very low cage contents, the thermomechanical properties of the oxidized epoxystannoxane resins, which are stabilized (or even reinforced) by the cross-linking reactions of the cages, approach the thermomechanical properties of the neat matrix after standard cure (Figure 17). For comparison, the neat matrix nearly degrades to a liquid after the mentioned oxidation treatment. While the resins with high stannoxane loadings become hard and brittle after the oxidation, the ones with low cage contents display mechanical properties similar to the original matrix not only after the standard cure but also after the oxidation.

The lower limit concentrations of Sn₀, Sn2, and Sn4, which are needed to approximately preserve the thermomechanical properties of the epoxy resin, are evaluated in Figure 17: It can

be seen that the highest stabilizing effect is achieved by the Sn₂ and Sn₀ cages, among which Sn₂ is slightly more efficient. Both stannoxanes achieve a very good matrix stabilization at 1 wt %, while 4 wt % are needed in the case of Sn₄ for a similar result. The higher efficiency of Sn₀ and Sn₂ is obviously due to their better accessibility for cross-linking reactions, which they possess as freely dispersed molecules (Sn₀) or as linear segments in the matrix structure (Sn₂). If the resins containing 1 wt % of Sn₀ or Sn₂ are subjected to a prolonged oxidation treatment at 180 °C for 30 days (results being prepared for publication), they do not degrade to a liquid (as does the neat matrix after 12–18 h) but they slowly lose weight (organic matrix “combustion”) and become stronger reinforced and finally brittle, as the content of the inorganic phase increases.

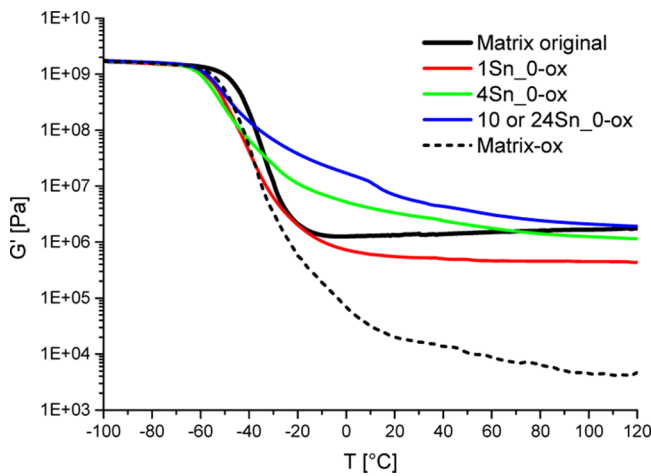


Figure 16. Effect of Sn₀ content on the thermomechanical properties of the epoxy-Sn₀ resins which underwent oxidation treatment: shear storage modulus G' as a function of temperature. The cage content is in the range of 1–10 wt %. The DMTA profile of the neat matrix after analogous oxidation treatment is shown for comparison.

3.4.3. Comparison of Stannoxane and POSS Cages’ Stabilizing Effect. The stabilizing effects of the stannoxane cages and of their lighter POSS homologue in the DGEBA-D2000 matrix are compared in Figures 18 and 19, under the conditions of annealing and oxidation, which were used in this work. A sample with 4 wt % Sn₀, which is already very efficiently stabilized against oxidation (a similar but slightly stronger effect is achieved by Sn₂), is compared with a modified DGEBA-D2000 resin, which is highly efficiently mechanically reinforced by 33 mol % (27 wt %) CpPOSSdgeba, incorporated as epoxy comonomer. After the standard cure, a distinct physical cross-linking by POSS is observed (higher rubber modulus), in comparison to a slight reinforcement by Sn₀ (very small increase in T_g and rubber modulus).

After annealing under argon, which causes thermal degradation of the matrix (see Figures 18 and 19), the mechanical properties of the hybrid resins containing Sn₀ and CpPOSSdgeba deteriorate due to the matrix degradation, which manifests itself as rubber modulus decrease. In the case of the POSS composite, the degradation is less pronounced than in the case of the neat matrix: POSS at 33 mol % (27 wt %) hinders the anaerobic probably via hindering the segmental mobility of the matrix. On the other hand, Sn₀ (at 4 wt %) does not hinder the anaerobic matrix degradation, which occurs approximately to the same extent like in the neat matrix. In contrast to Sn₀, the chemically bonded cages Sn₂

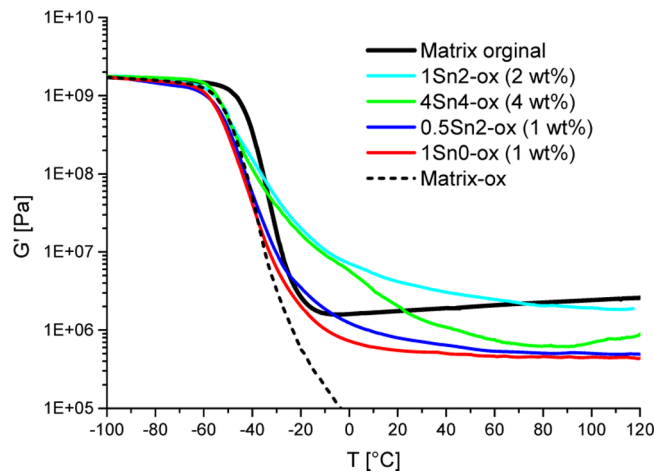


Figure 17. Proof of the highest antioxidative activity of “Sn₂”: Comparison of the DMTA profiles of oxidized epoxystannoxane resins with a low cages’ content: 1-Sn₂-ox (2 wt %), 4-Sn₄-ox (4 wt %), 0.5-Sn₂-ox (1 wt %), and 1-Sn₀-ox (1 wt %): Shear storage modulus G' as a function of temperature.

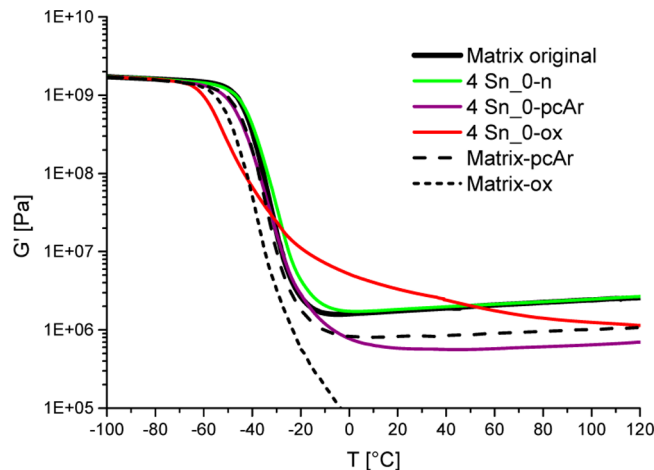


Figure 18. Thermomechanical properties ($G' = f(T)$ curves) of the DGEBA-D2000 matrix efficiently stabilized by 4 wt % Sn₀ after standard cure, after additional annealing under argon and after additional oxidation treatment, in comparison with the neat matrix in the same situations; Sn₂ achieves an analogous but somewhat better effect already at 2 wt %.

and especially Sn₄ hinder the matrix degradation more efficiently, blocking it completely in some cases (see above, Figure 12).

After the standard oxidation treatment performed in this work, the mechanical properties of the neat DGEBA-D2000 matrix radically deteriorate (Figures 18 and 19). The mechanical properties of the CpPOSSdgeba reinforced composite also deteriorate after this treatment, but to a much smaller extent than the neat matrix. Like in the case of the anaerobic degradation, the hindering of segmental mobility in the matrix by the large amount of POSS is the mechanism of this effect. In contrast to POSS, Sn₀ at 4 wt % effectively protects the matrix against the oxidative degradation of its mechanical properties, via the above-discussed oxidative cross-linking reactions. 2 wt % of the linearly bonded Sn₂ is needed for a similar effect like with 4 wt % Sn₀ (see above Figure 17), while the branching Sn₄ is less efficient than both Sn₂ and Sn₀ (Figure 17).

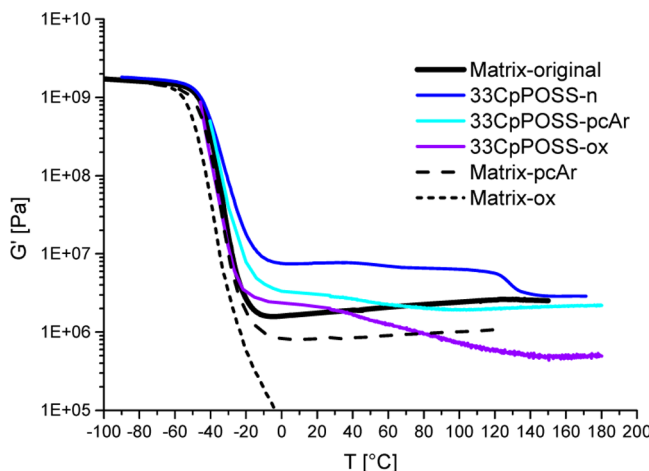


Figure 19. Thermomechanical properties ($G' = f(T)$ curves) of the DGEBA-D2000 matrix efficiently mechanically reinforced by 27 wt % CpPOSSdgeba after standard cure, after additional annealing under argon, and after additional oxidation treatment, in comparison with the neat matrix in the same situations.

While POSS was shown in this work to be inferior to stannoxane in preventing oxidative matrix degradation under mild conditions, it is known from the literature to be an efficient fire retardant,⁶⁰ and its protective effect in organic matrices against atomic oxygen (AO) in low Earth orbit conditions is one of the prospective future applications of POSS.^{46,61} In the latter case, a surface layer of the POSS-reinforced polymer is degraded by AO, but the POSS units from this layer form a passivating SiO_2 layer, which protects the deeper layers of the material from AO attack. In the case of stannoxane cages, their eventual suitability as fire retardants or as additives in space survivable materials has to be investigated in the future.

4. CONCLUSIONS

1. Organic–inorganic epoxy resins were prepared by incorporating the heavier POSS homologue, *n*-butylstannoxane dodecamer in different bonding situations, as a free inorganic cage (molecularly blended), as a linear, and as a branching unit (comonomer).

2. Similarly like nonbonded POSS, the nonbonded stannoxane cage (“Sn₀”) tends to phase separation during the later stages of matrix synthesis. Nevertheless, at a small concentration, the nonbonded stannoxane remains homogeneously dispersed and achieves a highly efficient antioxidative stabilization of the matrix.

3. The stannoxane cage incorporated as linear unit (comonomer, “Sn₂”) displays the fastest incorporation in the epoxy matrix due to the high reactivity of its amino groups. It is very finely dispersed and possesses some segmental mobility due to its bonding situation. Consequently, this building block displays the highest chemical reactivity, both in antioxidative cross-linking reactions and in cage polymerization reactions.

4. The linearly bonded Sn₂ cage exhibits a remarkable short-range mobility in the matrix at elevated temperatures in the absence of oxygen. This mobility leads to an unusual nanophase separation during anaerobic annealing, while at room conditions, the Sn₂ cage is bonded to the matrix and is not extractable. This interesting effect is connected with the oxonium ionic bonds which attach the functional substituents to Sn₂, especially with the reversibility (dissociation) of these

bonds at elevated temperatures (as investigated by NMR and IR). Structures with oxonium or ammonium bonds similar to those in Sn₂ might be of interest as materials displaying reversible chemical bonding.

5. The amino-H-four-functional stannoxane “Sn₄”, which bonds as a branching unit (comonomer), displays a slow incorporation into the forming matrix, due to the low reactivity of its aromatic amino groups. This cage is attached in the later reaction stages, which in turn leads to the earlier reported complex phase structure of the epoxy-Sn₄ resin (small primary and loose secondary aggregates). The “Sn₄” cage displays a fair antioxidative activity, which is nevertheless markedly lower than in case of its linearly bonded analogue, “Sn₂” or of nonbonded “Sn₀”. Because of the complex morphology, the polymerization of “Sn₄” in the primary domains does not change the phase structure of the epoxy-Sn₄ resin, neither does it change significantly the mechanical properties. On the other hand, due to its high amino-H-functionality, the “Sn₄” cage (comonomer) causes by far the strongest mechanical reinforcement of the epoxy matrix among the investigated stannoxane cages.

■ ASSOCIATED CONTENT

S Supporting Information

Figures 1–8. This material is available free of charge via the Internet at <http://pubs.acs.org>.

■ AUTHOR INFORMATION

Corresponding Author

*Tel (+420) 296 809 384; e-mail strachota@imc.cas.cz (A.S.).

Notes

The authors declare no competing financial interest.

■ ACKNOWLEDGMENTS

The authors thank Czech Science Foundation, grant 108/11/2151, for the financial support of this work. The authors also thank Ms. Dana Kaňková for recording NMR spectra as well as Ms. Miroslava Brunclíková (ATR-FTIR), Ms. Jiřina Hromádková (electron microscopy), Ms. Eva Miškovská (X-ray scattering), Ms. Zuzana Walterová, and Ms. Zuzana Kálalová for the determination of the tin content via ash analysis.

■ REFERENCES

- (1) Wu, J.; Mather, P. T. *Polym. Rev.* **2009**, *49*, 25–63.
- (2) Rubinstein, M.; Colby, R. H. *Polymer Physics*; Oxford University Press: Oxford, 2003.
- (3) Miri, V.; Elkoun, S.; Peurton, F.; Vanmansart, C.; Lefebvre, J. M.; Krawczak, P.; Seguela, R. *Macromolecules* **2008**, *41*, 9234–9244.
- (4) Trece, M. A.; Oberhauser, J. P. *Macromolecules* **2007**, *40*, 571–582.
- (5) Spirkova, M.; Brus, J.; Hlavata, D.; Kamisova, H.; Matejka, L.; Strachota, A. *Surf. Coat. Int., Part B* **2003**, *86*, 187–193.
- (6) Zhou, W.; Yu, Y.; Chen, H.; DiSalvo, F. J.; Abruna, H. D. *J. Am. Chem. Soc.* **2013**, *135*, 16736–16743.
- (7) Matteucci, S.; Van Wagner, E.; Freeman, B. D.; Swinne, S.; Sakaguchi, T.; Masuda, T. *Macromolecules* **2007**, *40*, 3337–3347.
- (8) Weng, C. J.; Huang, J. Y.; Huang, K. Y.; Jhuo, Y. S.; Tsai, M. H.; Yeh, J. M. *Electrochim. Acta* **2010**, *55*, 8430–8438.
- (9) Miniewicz, A.; Girones, J.; Karpinski, P.; Mossety-Leszczak, B.; Galina, H.; Dutkiewicz, M. *J. Mater. Chem. C* **2014**, *2*, 432–440.
- (10) Rao, Y. Q.; Chen, S. *Macromolecules* **2008**, *41*, 4838–4844.
- (11) Kuila, B. K.; Park, K.; Dai, L. M. *Macromolecules* **2010**, *43*, 6699–6705.
- (12) Kim, H.; Abdala, A. A.; Macosko, C. W. *Macromolecules* **2010**, *43*, 6515–6530.

- (13) Moniruzzaman, M.; Winey, K. I. *Macromolecules* **2006**, *39*, 5194–5205.
- (14) Hammond, M. R.; Dietsch, H.; Pravaz, O.; Schurtenberger, P. *Macromolecules* **2010**, *43*, 8340–8343.
- (15) Horak, D.; Babic, M.; Jendelova, P.; Herynek, V.; Trchova, M.; Likavcanova, K.; Kapcalova, M.; Hajek, M.; Sykova, E. *J. Magn. Magn. Mater.* **2009**, *321*, 1539–1547.
- (16) Priolo, M. A.; Gamboa, D.; Holder, K. M.; Grunlan, J. C. *Nano Lett.* **2010**, *10*, 4970–4974.
- (17) Kim, H.; Macosko, C. W. *Macromolecules* **2008**, *41*, 3317–3327.
- (18) Spirkova, M.; Strachota, A.; Urbanova, M.; Baldrian, J.; Brus, J.; Slouf, M.; Kuta, A.; Hrdlicka, Z. *Mater. Manuf. Processes* **2009**, *24*, 1185–1189.
- (19) Spirkova, M.; Brus, J.; Brozova, L.; Strachota, A.; Baldrian, J.; Urbanova, M.; Kotek, J.; Strachotova, B.; Slouf, M. *Prog. Org. Coat.* **2008**, *61*, 145–155.
- (20) Dal Pont, K.; Gérard, J. F.; Espuche, E. *J. Polym. Sci., Part B: Polym. Phys.* **2013**, *51*, 1051–1059.
- (21) Xu, Z.; Gao, C. *Macromolecules* **2010**, *43*, 6716–6723.
- (22) Yu, J. C.; Tonpheng, B.; Grobner, G.; Andersson, O. *Macromolecules* **2012**, *45*, 2841–2849.
- (23) Spirkova, M.; Strachota, A.; Strachotova, B.; Urbanova, M. *Surf. Eng.* **2008**, *24*, 268–271.
- (24) Oleksy, M.; Galina, H. *Ind. Eng. Chem. Res.* **2013**, *52*, 6713–6721.
- (25) Matějka, L.; Strachota, A.; Pleštil, J.; Whelan, P.; Steinhart, M.; Slouf, M. *Macromolecules* **2004**, *37*, 9449–9456.
- (26) Strachota, A.; Kroutilová, I.; Kovářová, J.; Matějka, L. *Macromolecules* **2004**, *37*, 9457–9464.
- (27) Strachota, A.; Whelan, P.; Kříž, J.; Brus, J.; Urbanová, M.; Šlouf, M.; Matějka, L. *Polymer* **2007**, *48*, 3041–3058.
- (28) Brus, J.; Urbanova, M.; Strachota, A. *Macromolecules* **2008**, *41*, 372–386.
- (29) Eychenne-Baron, C.; Ribot, F.; Steunou, N.; Sanchez, C. *Organometallics* **2000**, *19*, 1940–1949.
- (30) Ribot, F.; Escax, V.; Martins, J. C.; Biesemans, M.; Ghys, L.; Verbruggen, I.; Willem, R. *Chem.—Eur. J.* **2004**, *10*, 1747–1751.
- (31) Van Lokeren, L.; Willem, R.; van der Beek, D.; Davidson, P.; Morris, G. A.; Ribot, F. *J. Phys. Chem. C* **2010**, *114*, 16087–16091.
- (32) Puff, H.; Reuter, H. *J. Organomet. Chem.* **1989**, *373*, 173–178.
- (33) Dakternieks, D.; Zhu, H.; Tiekkink, E. R. T.; Colton, R. J. *J. Organomet. Chem.* **1994**, *476*, 33–38.
- (34) Chandrasekhar, V.; Gopal, K.; Singh, P.; Narayanan, R. S.; Duthie, A. *Organometallics* **2009**, *28*, 4593–4601.
- (35) Holmes, R. R. *Acc. Chem. Res.* **1989**, *22*, 190–194.
- (36) Ribot, F. In *Tin Chemistry: Fundamentals, Frontiers, and Applications*; Davies, A. G., Gielen, M., Pannell, K. H., Tiekkink, E. R. T., Eds.; Wiley: Chichester, 2008; pp 69–92.
- (37) Eychenne-Baron, C.; Ribot, F.; Steunou, N.; Sanchez, C. *J. Organomet. Chem.* **1998**, *567*, 137–142.
- (38) Ribot, F.; Banse, F.; Diter, F.; Sanchez, C. *New J. Chem.* **1995**, *19*, 1145–1153.
- (39) Ribot, F.; Lafuma, A.; Eychenne-Baron, C.; Sanchez, C. *Adv. Mater.* **2002**, *14*, 1496–1499.
- (40) Ribot, F.; Veautier, D.; Guillaudeau, S. J.; Lalot, T. *J. Mater. Chem.* **2005**, *15*, 3973–3978.
- (41) Strachota, A.; Ribot, F.; Matějka, L.; Whelan, P.; Starovoytova, L.; Pleštil, J.; Steinhart, M.; Slouf, M.; Hromadkova, J.; Kovarova, J.; Spirkova, M.; Strachota, B. *Macromolecules* **2012**, *45*, 221–237.
- (42) Ribot, F.; Sanchez, C.; Willem, R.; Martins, J. C.; Biesemans, M. *Inorg. Chem.* **1998**, *37*, 911–917.
- (43) Cordes, D. B.; Lickiss, P. D.; Rataboul, F. *Chem. Rev.* **2010**, *110*, 2081–2173.
- (44) Tanaka, K.; Chujo, Y. *J. Mater. Chem.* **2012**, *22*, 1733–1746.
- (45) Kuo, S. W.; Chang, F. C. *Prog. Polym. Sci.* **2011**, *36*, 1649–1696.
- (46) Phillips, S. H.; Haddad, T. S.; Tomczak, S. J. *Curr. Opin. Solid State Mater. Sci.* **2004**, *8*, 21–29.
- (47) Li, G.; Wang, L.; Ni, H.; Pittman, C. U. *J. Inorg. Organomet. Polym.* **2001**, *11*, 123–154.
- (48) Xiao, F.; Sun, Y. Y.; Xiu, Y. H.; Wong, C. P. *J. Appl. Polym. Sci.* **2007**, *104*, 2113–2121.
- (49) Liu, Y.; Zheng, S.; Nie, K. *Polymer* **2005**, *46*, 12016–12025.
- (50) Choi, J.; Harcup, J.; Yee, A. F.; Zhu, Q.; Laine, R. M. *J. Am. Chem. Soc.* **2001**, *123*, 11420–11430.
- (51) Gnanasekaran, D.; Madhavan, K.; Reddy, B. S. R. *J. Sci. Ind. Res.* **2009**, *68*, 437–464.
- (52) Pistor, V.; Ornaghi, F. G.; Ornaghi, H. L.; Zattera, A. *J. Mater. Sci. Eng. A* **2012**, *532*, 339–345.
- (53) Abad, M. J.; Barral, L.; Fasce, D. P.; Williams, R. J. *J. Macromolecules* **2003**, *36*, 3128–3135.
- (54) Zucchi, I. A.; Galante, M. J.; Williams, R. J. J.; Franchini, E.; Galy, J.; Gerard, J. F. *Macromolecules* **2007**, *40*, 1274–1282.
- (55) Romo-Uribe, A.; Mather, P. T.; Haddad, T. S.; Lichtenhan, J. D. *J. Polym. Sci., Part B: Polym. Phys.* **1998**, *36*, 1857–1872.
- (56) Lee, A.; Lichtenhan, J. D. *Macromolecules* **1998**, *31*, 4970–4974.
- (57) Joshi, M.; Butola, B. S.; Simon, G.; Kukaleva, N. *Macromolecules* **2006**, *39*, 1839–1849.
- (58) Fu, B. X.; Gelfer, M. Y.; Hsiao, B. S.; Phillips, S.; Viers, B.; Blanski, R.; Ruth, P. *Polymer* **2003**, *44*, 1499–1506.
- (59) Baldi, F.; Bignotti, F.; Fina, A.; Tabuani, D.; Ricco, T. *J. Appl. Polym. Sci.* **2007**, *105*, 935–943.
- (60) Franchini, E.; Galy, J.; Gerard, J. F.; Tabuani, D.; Medici, A. *Polym. Degrad. Stab.* **2009**, *94*, 1728–1736.
- (61) Brunsvold, A. L.; Minton, T. K.; Gouzman, I.; Grossman, E.; Gonzalez, R. *High Perform. Polym.* **2004**, *16*, 303–318.